LAPPEENRANTA UNIVERSITY OF TECHNOLOGY
LUT School of Energy Systems
LUT Mechanical Engineering

Veli-Matti Valtonen

REAL-TIME MONITORING OF LASER SCRIBING PROCESS WITH PHOTODIODES

Examiners: Professor Antti Salminen
D. Sc. Hamid Roozbahani

ABSTRARCT

Lappeenranta University of Technology
LUT School of Energy Systems
LUT Mechanical Engineering

Veli-Matti Valtonen

Real-time monitoring of laser scribing process with photodiodes

Master's Thesis

2017

76 pages, 51 figures, 11 tables and 1 appendix

Examiners: Professor Antti Salminen
D.Sc. (Tech.) Hamid Roozbahani

Keywords: laser scribing, micromachining, monitoring, real-time, photodiode

The use of laser scribing as a method of material processing is growing in popularity within industrial applications. Especially in areas requiring extreme levels of accuracy. Laser scribing technology promises to offer improvements in many fields. A field of special interest is the manufacturing of solar cells, with improved efficiency in both manufacture and function. The high-quality requirement and fast speed of a laser scribing process, presents a requirement for monitoring the processes in real time in order to detect possible defects as early as possible in the manufacturing process. There is a distinct lack of research in the monitoring of laser scribing. Commonly available monitoring systems that have been developed for use in other laser based processes, such a laser welding, which tend to be significantly slower, thus they are not applicable to laser cribbing The goal of this thesis is to explore a the possibilities of using photodiodes for monitoring a laser scribing process. The laser in these experiments is an IPG ytterbium pulsed fiber laser that has a maximum average power of 20 W. The optical scan head used with the laser is Scanlab's Hurryscan 14 II equipped with an f100 telecentric lens. Commercially available photodiodes and laser pointers are used for probing the test scribes. Various configuration for monitoring the resulting scribes will be tested to determine which, if any is a viable option for implementing a monitoring application. The key obstacles will be identified and possible solutions will be considered. There are a couple of obstacles for this method of monitoring. Following such a precise process at the high speeds at which the scribing happens with adequate accuracy is extremely difficult. The monitoring illumination should provide enough contrast between material layers to be distinct, and to eliminate as much outside interference as possible. The study was successful in identifying the key aspects of developing such an application. Some success was achieved in measuring defects in stationary and slow moving tests, and a clear direction is pointed for future development. For an operational solution an optimal photodiode and monitoring beam combination should be selected and combined with a setup that allows for following the scribing process at operational speeds. This would still be limited to processing materials with enough reflective contrast between layers.

TIIVISTELMÄ

Lappeenrannan teknillinen yliopisto
LUT School of Energy Systems
LUT Kone

Veli-Matti Valtonen

Laserkaiverrus prosessin reaaliaikainen valvonta fotodiodeilla

Diplomityö

2017

76 sivua, 51 kuvaa, 11 taulukkoa ja 1 liite

Tarkastajat: Professori Antti Salminen
TkT Hamid Roozbahani

Avainsanat: laserkaiverrus, laser mikrotyöstö, reaaliaika valvonta, virheen tunnistus

Laserkaiverrus on materiaalityöstö menetelmä, jonka suosio teollisuudessa kasvaa nopeasti. Erityisesti alueilla joilla vaaditaan äärimmäistä tarkkuutta. Laserkaiverrus tarjoa etuja useilla alueilla. Erityisen kiinnostava alue on aurinkokennojen valmistus, jossa voidaan saavuttaa parempia hyötysuhteita, sekä valmistuksessa että käytössä. Korkeat laatuvaatimukset ja suuret työstönopeudet luovat tarpeen reaaliaikaiselle valvonnalle, joka pystyy havaitsemaan virheet mahdollisimman nopeasti. Laserkaiverruksen valvonta on huomattavan vähän tutkittu aihe. Yleisesti saatavilla olevat valvontajärjestelmät ovat kehitetty prosesseja, kuten laserhitsausta varten, ja ne eivät hitautensa vuoksi sovellu laserkaiverruksen valvontaa. Tämän tutkimuksen tavoitteena on tarkastella mahdollisuuksia käyttää fotodiodeja laserkaiverrus prosessin valvontaan. Kokeissa käytetty laser oli IPG yttebrium pulssitettu kuitu laser, jonka maksimi keskiteho oli 20 W:n. Suuntaus optiikkana käytettiin Scanlabin Hurryscan 14 II laser skanneria, joka oli varustettu f100 telesentrisellä linssillä. Testikaiverrusten mittaukseen käytetään kaupallisesti saatavilla olevia fotodiodeja ja laser pointtereita. Eri valvonta konfiguraatioita testataan, jotta saadaan selville onko mikään niistä käyttökelpoinen valvontasovelluksen kehitystä varten. Tutkimuksessa tunnistetaan fotodiodi valvonnan avain haasteet ja tarjotaan niihin mahdollisia ratkaisuja. Tämän tyyppiselle valvonnalle on olemassa muutamia haasteita. Niin tarkan ja nopeasti liikkuvan prosessin seuraaminen riittävällä tarkkuudella on erittäin haastavaa. Valvontavalaisun tulisi mahdollistaa riittävän selkeä kontrastiero materiaalikerrosten välillä ja sulkea pois mahdollisimman paljon ulkoisia häiriöitä. Tutkimuksessa onnistuttiin selvittämään valvontasovelluksen kehityksen avain haasteet. Jonkin verran menestystä saavutettiin mittaamalla virheitä paikallan olevista tai hitaasti liikkuvista testikappaleista ja jatkokehitykselle osoitettiin selkeä suunta. Toimivaa ratkaisua varten olisi valittava optimaalinen fotodiodi valvonta laser yhdistelmä, ja yhdistettävä se asetelmaan, joka pystyy luotettavasti seuraamaan prosessia käyttönopeuksissa. Tämä kuitenkin rajoittuisi materiaaleihin, jotka tarjoavat tarpeeksi heijastavuus kontrastia aine kerroksien välillä.

ACKNOWLOEDGEMENTS

This research is a part of the APPOLO-project funded by the European Union, and it is conducted in Lappeenranta University of Technology (LUT) Laboratory of Laser Processing (LUT Laser). LUT Laser activities were conducted as a part of Work Package 8 of the project. APPOLO is a collaborative project between several European universities and research institutes. The research is focused on new laser processing applications which need to be customized, tested and validated for commercial use. One major goal of the APPOLO-project is the evaluation of the benefits of using photodiodes in the on-line monitoring of laser scribing.

I want to acknowledge the examiners of my thesis, Professor Antti Salminen and Doctor Hamid Roozbahani for allowing me to have an opportunity to work on such a uniquely interesting project and collaborate with professionals from various fields on an international level. I would like to extend my gratitude to them for their assistance and for providing me with the tools to conduct this project. I especially want to thank Doctor Hamid Roozbahani for his tireless dedication to the project and for the learning opportunities he provided. I also want to extend my thanks to my co-workers, Mika Ruutiainen and Pekka Marttinen for their input and assistance, Ilkka Poutiainen and Pertti Kokko for providing technical support and Matti Manninen for guidance in the operation of the laser.

I would also wish to give thanks to my fellow students and the staff of the University for All of their support.

Veli-Matti Valtonen

Veli-Matti Valtonen

Lappeenranta 21.5.17

TABLE OF CONTENTS

ABSTRACT

ACNOWLEDGEMENTS

TABLE OF CONTENTS

LIST OF ABBREVITATIONS

1 INTRODUCTION 9

2 BACKGROUND 11

3 APPOLO 13

3.1 Segments of the project 16

4 BASICS OF MACHINE VISION 17

4.1 Photodiode sensors 17

4.2 Physics of photodiodes 18

4.3 Control Theory 21

4.3.1 On-line monitoring 21

4.3.2 Real-time Control System 22

4.4 Open-loop control system 22

4.5 Closed-loop control system 22

4.6 Typical Monitoring Systems 23

4.7 Intelligent Data Acquisition System 23

4.8 Control design methodology 24

5 BASICS OF LASER SCRIBING IN MATERIAL PROCESSING 26

5.1 Ultrafast lasers in solar panel manufacturing applications 28

6 EXISTING PHOTODIODE MONITORING APPLICATIONS FOR LASER PROCESSES 29

6.1 Laser Welding Monitor 29

6.2 System description of the Laser Welding Monitor LWM 30

6.3 Configuration examples 30

6.4 Technical Data 31

6.5 Laser Power Control 32

7 TEST SETUP 34

7.1 Pulse laser 35

7.1.1 Optical characteristics 35
7.1.2 Optical Output 36
7.1.3 Electrical Characteristics 36
7.1.4 General Characteristics 36
7.1.5 Control Interfaces, configuration and operating modes 37
7.1.6 RS-232C electrical connector 40
7.1.7 Laser Control Software 40
7.2 Scan Head 41
7.2.1 Control Boards 43
7.3 Camera Adapter 45
7.3.1 Installation 46
7.3.2 Operating principle 47
7.4 Industrial computer (PXI-system) 48
7.4.1 PXIe Real Time module 50
7.4.2 NI BNC-2120 connector block 50
7.4.3 NI PXIe-6363 DAQ card 55
7.4.4 1103P Helium Neon Monitoring laser 56
7.5 LabVIEW System Design Software 58
8 EXPERIMENTS 59
8.1 Specular and Diffuse Reflection 59
8.2 CIGS Layer Distinction 61
8.3 Monitoring Setup Experiments 62
9 EXPERIMENTAL RESULTS 64
9.1 PRECITEC LWM tests 64
9.2 Specular and Diffuse reflection 65
9.3 CIGS Layer Distinction 67
9.4 Monitoring Setup Experiments 67
10 ANALYSIS AND DISCUSSION 71
11 CONCLUSIONS AND SUMMARY 72
LIST OF REFERENCES 74
APPENDIX
APPENDIX I: Technical drawings

LIST OF ABBREVIATIONS

ASLR	address space layout randomization
BNC	Bayonet Neill-Concelman (connector)
BS	bit Stream
CIGS	copper indium gallium selenide
CPU	central processing unit
CW	continuous wave
DAQ	data acquisition
DLL	dynamic-link library
DSP	digital signal processor
EC	European Commission
EM	electromagnetic
HAZ	heat-affected zone
HC	high contrast
HMI	human-machine interface
ICT	information and communications technology
I/O	input/output
LabVIEW	laboratory virtual instrument engineering workbench
LED	light emitting diode
LIFT	laser-induced forward transfer
LWM	laser welding monitor
NI	National Instruments (company)
PCI	peripheral component interconnect
PID	proportional integral derivative (controller)
PLC	programmable logic controller
PRR	pulse repetition rate
PXI	PCI extension for instrumentation
RCS	real-time control system
RTC	real time control
SISO	single input single output
SM	system monitor

SME	small to medium sized company
VI	virtual instrument

1 INTRODUCTION

The use of ultrafast lasers provides many new possibilities for microscale processing applications due to their ability for virtually athermal ablation and high peak power. One particularly useful application is thin film laser scribing, which can be used for example in solar panel manufacturing in order to improve the efficiency of solar cells. Processing speed in laser scribing applications can reach as high as several meters per second, in combination with high quality requirements. Defects in the scribing line, resulting from disturbances in the process, will greatly affect the quality of the end product. Presently, there is a demand for research in the fields of process monitoring and quality control. Commonly used laser processes, such as laser welding are widely researched, and the technology for monitoring these processes is commonly used. However the operating speed of these types of processes are significantly lower than those used in laser scribing. This is why laser scribing requires a faster and more accurate monitoring system.

The goal of this study is to develop and evaluate a method for monitoring the laser scribing process in real time using photodiodes in order to detect defects in the process. In this context, a defect refers to a discontinuance in the scribing line. The high performance requirements set by the speed of the laser scribing process are the main challenges for real-time monitoring. An option for performing the monitoring, is to use photodiodes to observe the process and to detect anomalies in either the scribing process, or in the scribed line immediately behind the scribing event. National Instruments (NI) “Laboratory Virtual Instrument Engineering Workbench” (LabVIEW) system design software is the software used for programming and developing the monitoring algorithms and applications. The intention is to build a test setup for experimenting with the use photodiodes in defect detection. The feasibility and performance of the monitoring techniques will be evaluated with the use of practical experiments. This research is conducted as a part or the European Union funded APPOLO project.

In preparation for constructing the real-time monitoring system for a laser scribing process, some research is conducted in order to gather information on how monitoring is implemented in laser welding processes. In addition some research is conducted on the operation of photodiodes, machine vision and laser micromachining. This paper is comprised of two main sections; the theoretical section including the background of existing knowledge and the experimental section which includes the testing setup, along with the experiments and their results.

2 BACKGROUND

Scribe regularity and potential scribing errors are determined during optical and geometrical inspection. Variations in the pulse energy can occur on different time-scales. It can occur that one pulse has a significantly different energy, such as a missing pulse, or the variation can occur on a medium time-scale with hundreds of pulses involved or even slower, drifting away from the scribe parameters. For low overlap processes such as P1 and P3 already one sub-threshold pulse can create a shunt. In this case we can measure the number of sub-threshold pulses per million using a linear scale. For high overlap processes such as P2 one missing pulse does not significantly affect the scribe result, in which case we can measure the standard deviation in a short time window e.g. 100 pulses. Alternatively we can measure the number of consecutive pulses below a certain value or the number of sub-threshold pulses in a sample of 100 consecutive pulses.

It is very important to recognize these deflections during the scribing process of the solar panels. The main questions to answer is, if there is a scribing error during the process, then where is the defect located.

Testing the solar panels after production for quality control does not help, as the panel will be taken off the line and scrapped if defects are detected. It is important to detect the problem during the process and record the exact location. In this way, it is possible to scribe the defective point manually and salvage the panel.

A real-time monitoring system based on photodiodes could be utilized to solve the above-mentioned problem. In a monitoring system that operates in real-time, which provides online information of relevant quality about the laser scribing process, changes to scribing parameters could be detected and deviations in the scribe found while still on the production line. The scribing process “fingerprint” can be determined by the reference values obtained from a successful baseline scribe, which is compared to an active production signals, and analyzed in real time.

In-process monitoring self-sufficient real-time measuring system with non-contact signal recording and calculation capability adapted to the specific process depending on the scribing parameters, the monitoring system could information on defects such as: penetration depth, full depth, failures, spatter, etc. enabling process learning and, error correction where possible, allowing for process improvement and adaptation.

These requirements in the laser processing industry could be met with the proper monitoring solution. Improving product quality and lowering production costs by minimizing waste. When applied to solar cell manufacturing, these advances could provide greater possibilities in the field of green energy.

3 APPOLO

Lasers have been in existence for more than 50 years, and they have been proven to be a unique tool for diverse material processing applications. Laser technology can be utilized for various manufacturing applications, such as material processing. This technological diversity provides a good platform for innovative solutions in creating new products and process technologies and provides the tools to make them a reality. This broad field has been left open for relatively small European companies with focused expertise and accumulated knowledge in developing laser applications. The future of the manufacturing industry is of vital importance to Europe's economic prosperity and long term sustainability. Innovative new ideas need to be realized to form new innovative products and manufacturing processes.

The new ideas and application, which are being developed at universities as well as other research institutions have been, for the most part, realized in the form of spin-off companies which often have quite limited resources that could be used for achieving good market penetration. Most of the manufacturers in the field are small to medium sized companies (SME) and only a few of them have the required research capacity and adequate financial means to implement high-risk innovative manufacturing technologies. The European Commission (EC) and industrial organizations have a new support scheme for, the "Private-Public-Partnership initiative", "Factories of the Future", which is intended to be targeted at the manufacturing industry along with the development of new, sustainable and innovative technologies. (APPOLO Newsletter 2014.)

The APPOLO project, which was officially launched on the 1st. of September, in 2013 as a part of the European Commission's information and communications technology (ICT) initiative "ICT Innovations for Manufacturing SMEs". This initiative is meant to help establish connections and coordinate them, to achieve co-operation between the intended end-users that have a current or foreseeable demand for laser technologies that can be used in fabrication, the application laboratories operating in the universities and research institutes, which have an abundance of accumulated knowledge, and the manufacturers of the equipment used for novel laser products, including beam guidance and control devices. (APPOLO project website.) This operational integration is meant to serve the goal of

providing more rapid validation of the feasibility of a process and a shorter timespan for adapting the required equipment to accommodate the specific manufacturing requirements and conditions (APPOLO Newsletter 2014).

The assessment and evaluation process of these proprietary manufacturing technologies and applications are implemented thru the use of a “virtual hub of laser application laboratories” which includes research facilities that are located throughout Europe. These facilities can co-operatively accumulate knowledge and infrastructure, to provide for an easily accessible body of expertise and a good environment for developing and validating new technologies and applications that are based on laser technology. (APPOLO Newsletter 2014.)

The APPOLO project has an ambitious ultimate end goal, which is the establishment of a Laser Certification Center that can assist its partners operating in the European photonics industry to allow them to preserve their competitive position, while helping to find and effectively penetrate new niche markets available in the global marketplace (APPOLO project website). The aim of the project is to establish coordinated connections between the intended users of the applications, which have a requirement for laser based technology that can be used in areas such as microfabrication, the wealth of accumulate knowledge that is held by research institutes, university laboratories and manufacturers of the required laser equipment (APPOLO Newsletter 2014).

Preferred partners include SMEs focused on lasers, beam guidance and control technology, software, integration of technologies, etc. For facilitating quicker validation for the processes usability and adaptability or the customizing of the needed technology for the existing manufacturing conditions. This may ether in conjunction or separately include the customization and validation of equipment, including component reliability and the interaction of different components in the system. All of this is contained in the assessment of these proprietary manufacturing applications and processes, assessing them in terms of the speed of processing, product quality, system reliability and the repeatability of the process cycle. At the heart of this partnership are the laser “application laboratories” located on multiple sites all around Europe, which maintain their connection thru the use of the virtual hub, used to pool together their knowledge and their available infrastructure in order

to support an easily accessible working platform for the continued development and the reliable validation of new laser technology. (APPOLO project website.)

Figure 1, illustrates the structure of “APPOLO - Hub of Application Laboratories for Equipment Assessment in Laser Based Manufacturing”. Every one of the partner organizations have selected a few of the available directions or “clusters”, for their focus in the validation of new and innovative laser technology. These clusters include: equipment, such as the ultra-short pulse scribing laser that can be used for producing monolithic interconnections in copper indium gallium selenide (CIGS) solar cells, and can also be applied to laser to pilot line applications, utilizing lasers for smart-texturing of surfaces, which is useful in automotive and printing or decorating applications, as well as for flexible true-3D electronics. The innovative SMEs involved are connected and networked to the “large system-integrators” as well as the intended users through these interconnected “application laboratories”. (APPOLO project website.)

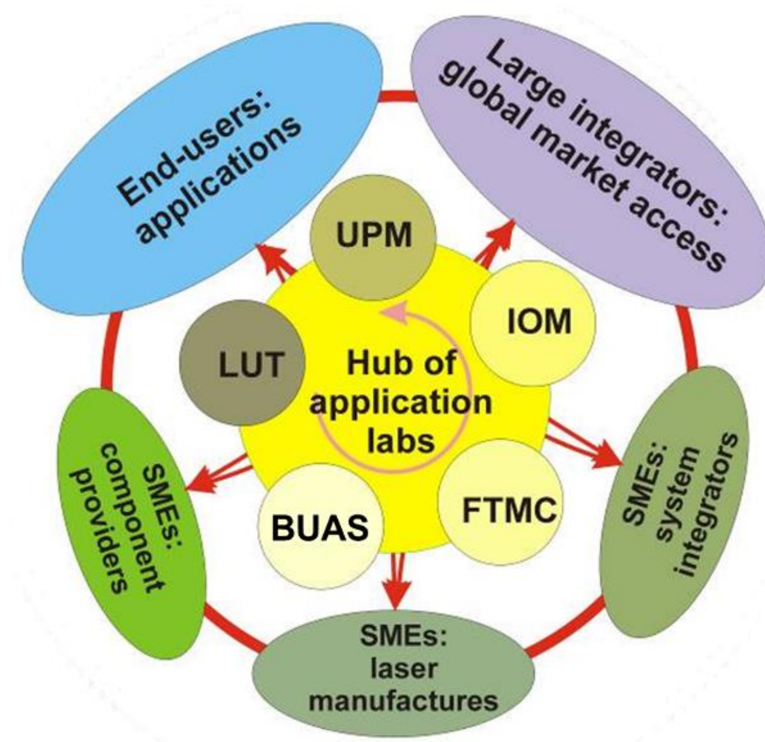

Figure 1. “APPOLO - Hub of Application Laboratories for Equipment Assessment in Laser Based Manufacturing” (APPOLO project website).

3.1 Segments of the project

The APPOLO project is divided in to six operational segments. Each segment is focused on a specified aspect of the project, allowing for greater focus on a specific project area and simplifying management and operational allocation. These project segments are listed below.

- CIGS scribing cluster: Assesses possible new processes and equipment for laser scribing of CIGS
- Texture cluster 1: Studying rapid structuring for printing and decoration applications
- Texture cluster 2: Surface engineering for producing functional finishes on surfaces
- Laser Direct Writing cluster 1: Producing 3D interconnections in polymer materials
- Laser Direct Writing cluster 2: Laser-induced forward transfer (LIFT) for use in photovoltaic Applications
- On-line monitoring tools

(APPOLO project website.)

4 BASICS OF MACHINE VISION

The defining principle machine vision is the integration of different censor technologies and computer analysis methods for providing usable information from visual inspection of the environment. Machine vision applications are widely implemented in industry, for example in sorting of items, handling of materials, making optical measurements, monitoring product quality guiding robots and automatic assembly lines and inspecting industrial operations. (Liu et al. 2015, p. 1-30.)

4.1 Photodiode sensors

A photodiode is a component consisting of an active p-n junction that is operating in a reversed bias. When the junction is exposed to light, a current flow is produced, which is in proportion to the illuminance. An illustration of this is shown in figure 2. This linear response to light provides an element which is useful in photodetector applications. (Nave 2012.)

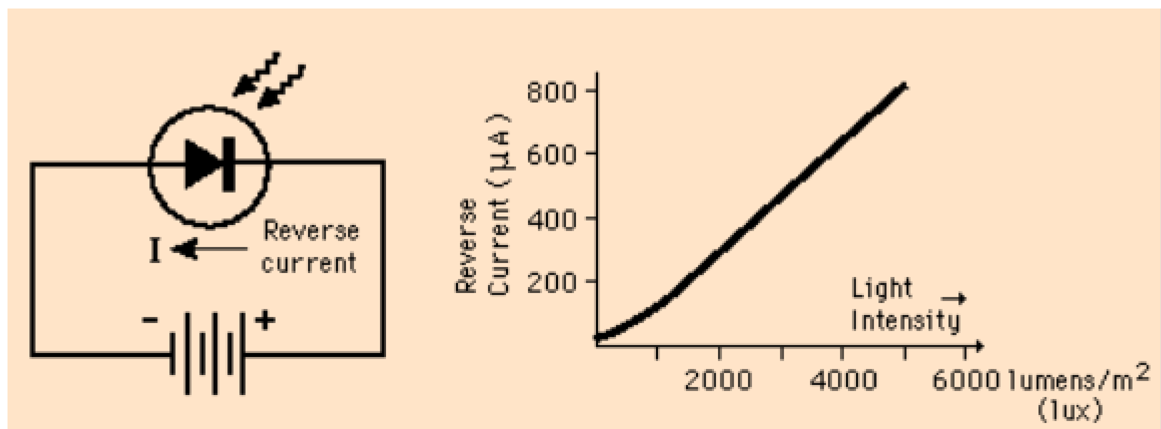

Figure 2. Photodiode diagram and current illuminance relationship (Nave 2012).

The operating principle of a photodiode is similar to that of a small solar cell. They have a fast response time that is operates in an order of nanoseconds. Functioning as a light detector, they are reversely biased with their reverse currents being linearly proportional to the incoming illuminance to which they are exposed to. While not as sensitive as phototransistor, the linear response makes them useful in simple light measuring applications. (Nave 2012.)

In a silicon photodiode incoming incidents light are converted into an electric current, thus it is functioning as a solid-state device. They are constructed as a shallow profile diffuse p-n junction, which is normally assembled in a p-on-n configuration, but “P-type” devices with an n-on-p configuration are also available for providing enhanced responsivity in the wavelength range of 1μm. Ion-implantation and planar diffusion are the methods which are most often used in the production of modern photodiodes. The planar diffused p-on-n configuration that is illustrated in figure 3, it can be seen that the edges of the junction emerge to the upper surface of the component, under an oxide layer that passivates it. (Photodiode Theory of Operation.)

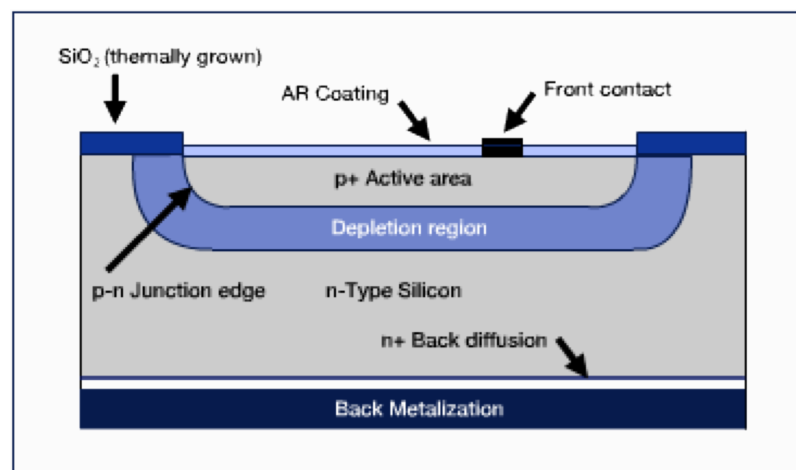

Figure 3. Silicon photodiode structure (Photodiode Theory of Operation).

4.2 Physics of photodiodes

According to the web article “Photodiode Theory of Operation” by AP Technologies: “The p-n junction and the depletion region are of major importance to the operation of a photodiode. These photodiode regions are created when the p-type dopant with acceptor impurities (excess holes), comes into contact with the n-type silicon, doped with donor impurities (excess electrons)”. These holes and electrons, experience a potential energy that is lower than that on the opposing end of the created junction, this causes them to flow to their respective areas of lower potential energy across the created junction. The resulting movement of an electric charge forms a depletion region that has its own electrical field, which is equal but opposite the field lower potential, thus stopping the current flow. (Photodiode Theory of Operation.)

When photons fall to the surface of the component, these are absorbed by the material, creating pairs of electrons and holes. The energy of the photons determines the depth to which they travel before being absorbed. The lower the photons energy is on impact, the deeper it will travel in the material before it is absorbed. The pairs of electrons and holes in the component start drifting away from each other, and upon reaching the junction, the electric field pulls the minority carriers across. When there is an electrical connection between these two sides, an external flow through of current can be produced in the connection. According to the web article “Photodiode Theory of Operation” by AP Technologies: “If the created minority carriers of that region recombine with the bulk carriers of that region before reaching the junction field, the carriers are lost and no external current flows”. (Photodiode Theory of Operation.)

A diagram of a circuit which is equivalent in operation to a photodiode is shown below in figure 4, the units in the figure are explained in table 1. When illuminated, photodiodes behave as sources current. When they are operating without any bias, the produced current is distributed equally in between the resistance of the external load and the internal shunt resistance. When operated in a mode such as this, it develops a voltage which results in a forward bias that reduces the circuit’s ability to produce a consistent flow of current. Alternatively, as mentioned in the web article “Photodiode Theory of Operation” by AP Technologies: “When operated with a reverse voltage bias, the photodiode becomes an ideal current source”. (Photodiode Theory of Operation.)

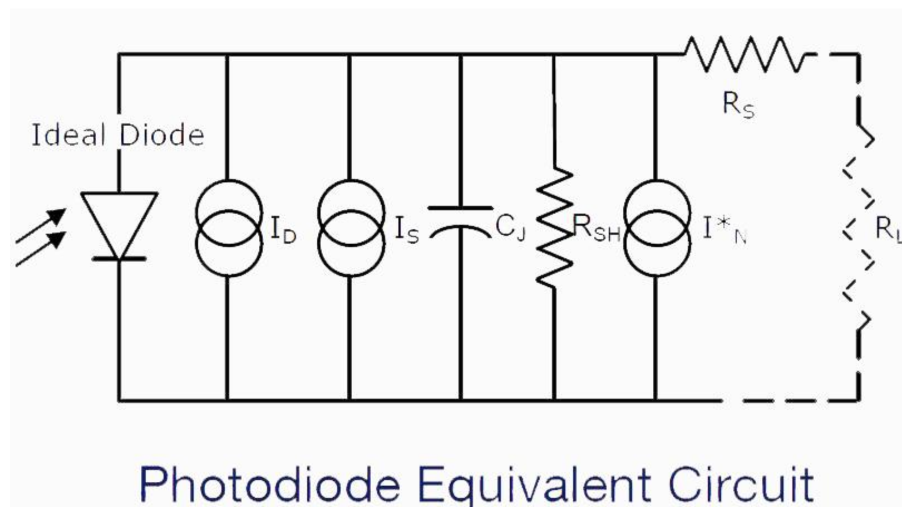

Figure 4. Photodiode equivalent circuit (Photodiode Theory of Operation). Units used are explained in table 1.

Table 1. Photodiode equivalent circuit units (Photodiode Theory of Operation). Used in figure 4.

I_D	Amount of dark current in Amperes
I_S	Light Signal Current (I_S=RP_O)
R	Photodiode responsivity at wavelength of irradiance in, Amperes/Watt
P_O	The power incident of light on the active area of the diode in Watts
R_{SH}	The Shunt Resistance in Ohms
I^*_N	Amount of Noise Current in Amperes rms
C	Capacitance of a Junction in Farads
R_S	The Series Resistance in Ohms
R_L	The Load Resistance in Ohms

Photodiodes made of silicon typically have a sensitivity to light in a range from approximately 200 nm, which is near ultraviolet, to approximately 1100 nm, which is near infrared. The responsiveness (R) of a photo sensor element is measured in units of Amperes (A) of generated photocurrent per Watt (W) of power of the incident light. The actual level of light that is used in most applications usually ranges in the order of pW to mW, this produces photocurrents in the order of pA to mA. Responsivity measured in Amperes/Watts varies significantly depending on the wavelength of the incoming incident light. The peak values for the responsiveness range from 0.4 to 0.7 A/W. The responsiveness obtained from a photodiode made of silicon is a good match for sources that emit light in a spectral range from ultraviolet to near infrared. Light sources that operate in that spectral range include HeNe lasers, Nd:YAG lasers and GaAs and GaAlAs light emitting diodes (LED) and laser diodes. The response of a silicon photodiode is generally linear in nature, from minute levels in the order of fractions of a percent above the minimum detection threshold of incident light power up to the level of multiple mW. The linearity of the response can be further improved by increasing the level of applied reverse bias and complementarily decreasing the applied effective load resistance. (Photodiode Theory of Operation.)

4.3 Control Theory

The field of Control theory is a branch of science that combines mathematics and engineering, focusing on dealing with the dynamic behavior of systems with inputs that are applied in order to cause the system variables to conform to desired values. Figure 5, illustrates a Single Input Single Output (SISO) system.

Figure 5. Single Input Single Output (SISO) system.

A system can have multiple inputs and outputs. Also both external and internal disturbances can affect the system as a type of unintended input. Figure 6, illustrates a system with multiple inputs and outputs including the effect of outside disturbances.

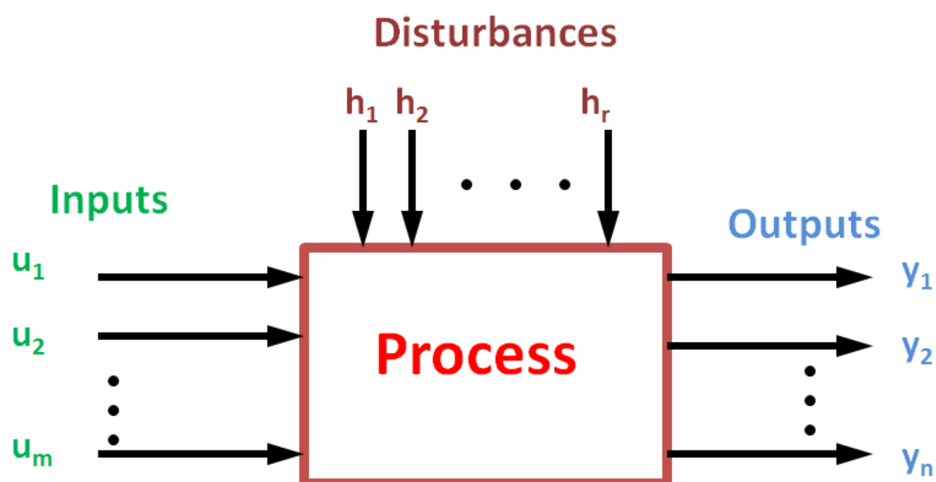

Figure 6. Diagram of a system with several inputs and outputs under effect of disturbances.

4.3.1 On-line monitoring

In the field system engineering, a system monitor (SM) is a process within a distributed system which enables the collection and storage of state data. This data can then be analyzed, distributed or archived, to be used as is necessary for the performance of the system.

For a device to be considered online, it must conform to one of the following criteria:

- It is directly controlled by another separate device
- It is directly controlled by a system that it is connected with
- It is immediately available for on-demand use by a system without intervention

4.3.2 Real-time Control System

A Real-time Control System (RCS) is a type of system architecture and methodology, used to develop an intelligent system out of several interconnected online sub systems.

4.4 Open-loop control system

An open-loop control system, which is also known as a non-feedback control system, is a category of controller that calculates the inputs it feeds into a system only using the system model and the current state in which it is initiated. Normally the available monitoring systems in laser industry have open loop control system. Figure 7, illustrates an open-loop control system.

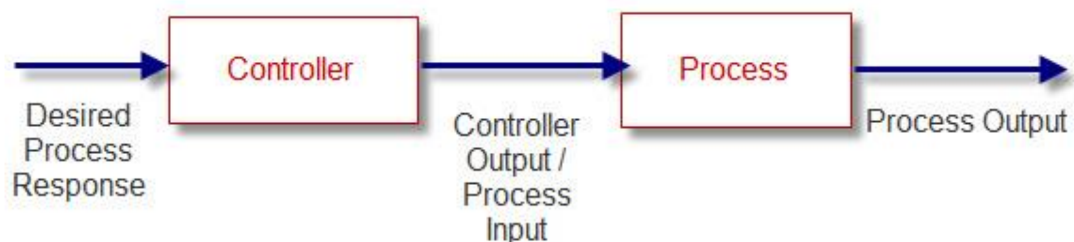

Figure 7. Diagram of an open-loop control system.

4.5 Closed-loop control system

A Closed-loop Control System, which is commonly known by its alternative name as a “feedback control system” is a category of controller that uses an open-loop system as its primary forward operating system path but as the name implies, it contains an integrated number of one or several feedback loops or rearward pathways between its outputs and its inputs. In this case the “feedback”, is quite simply a means for returning a specific section of an output as an input to a previous part of the system, in order to allow actual outputs to be utilized in adjusting the operation of the system. Figure 8, illustrates the operating principle of a closed-loop control system.

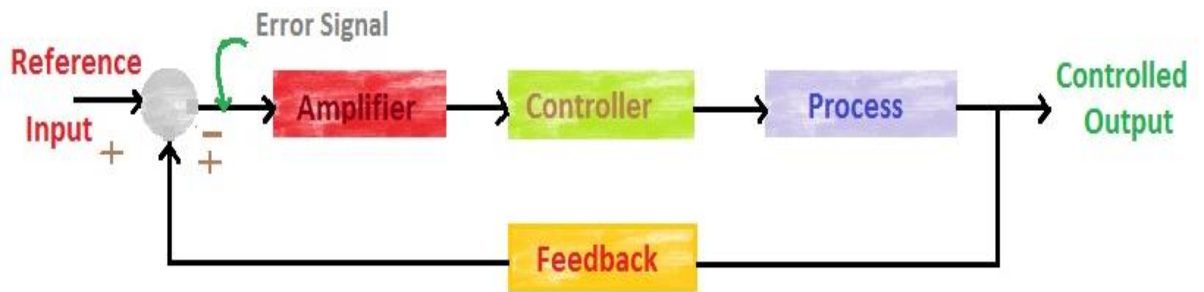

Figure 8. Diagram of a closed-loop control system.

4.6 Typical Monitoring Systems

A typical control system utilized in a laser application is equipped with an array of different sensors, but the system works based on an open loop control system. This means that all of the sensor data is saved by the operator and used to analyze the process separately. But this data is only used retroactively to tune the process in order to improve future operation. There is no feedback during the process to actively minimize process error. Figure 9, illustrates a typical process of laser monitoring based on an open loop control system.

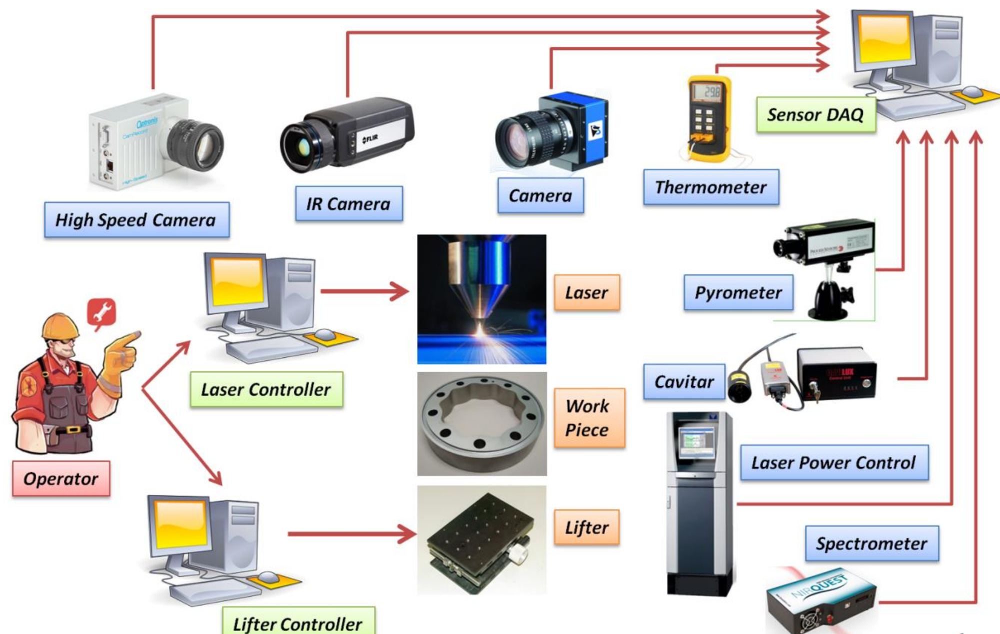

Figure 9. A typical process of laser monitoring based on open loop control system.

4.7 Intelligent Data Acquisition System

In an intelligent control system, most if not all of the sensor data is fed to a central control system, which can analyze the incoming data in practically real-time and can formulate the

best command to send to the laser in order to optimize the process, while it is in operation. Figure 10, illustrates the laser intelligent control system.

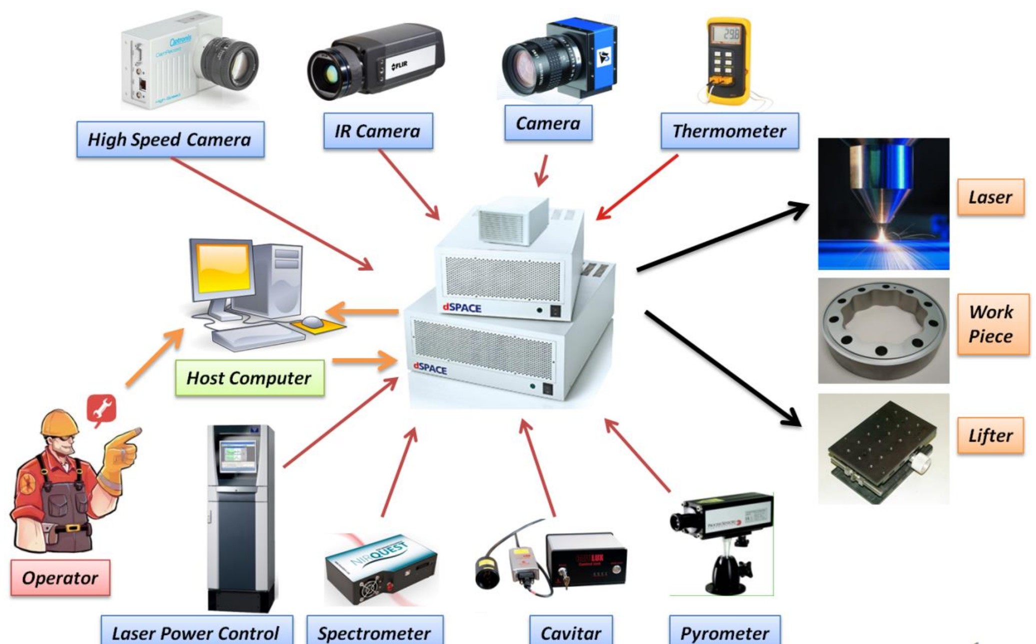

Figure 10. Laser intelligent control system.

4.8 Control design methodology

There is an increasingly active global approach and expanding requirement to design real-time control systems. The method for doing this begins with modeling the process. In this phase a mathematical model of the whole process is designed. This model simulates the behavior of the real process and it can be utilized to predict the action and reaction of the system, under different operating parameters. If this model is accurate and behaves the same as the real system based on same inputs, then it is dynamically the model simulator.

Based on this model a controller can designed, which can optimally adjust the process to achieve desired results. It can be a linear, a non-linear or just a control logic controller. Based on the mathematical methods used in control design, an algorithm is formulated in which the dynamics of the model are controlled to achieve the possible optimum point with minimal error. If the error of the system converges to zero then the controller called a satisfying controller. If it does not, then the controller design should be repeated to provide a better solution.

On the other hand, based on the requirements of the end user of the system, a requirement analysis is applied to the system and a standard test is designed to check and evaluate the final performance of the controller based on the user requirements. And all of the performance specifications are recorded for use in future controller design processes. Figure 11, illustrated the controller design process.

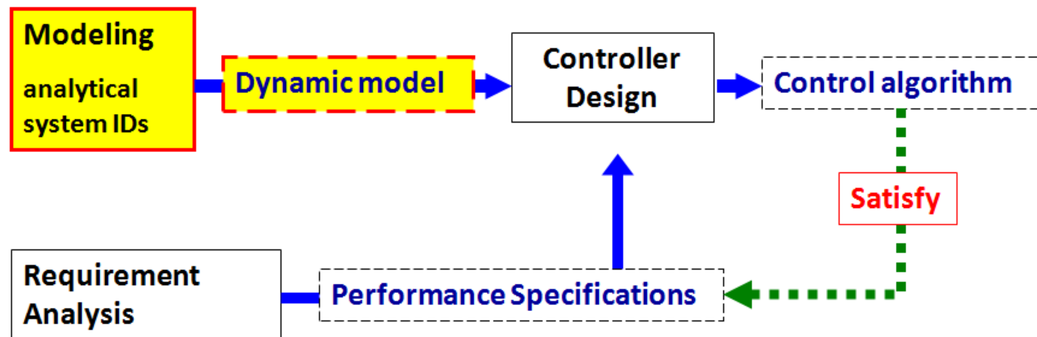

Figure 11. Controller design process.

5 BASICS OF LASER SCRIBING IN MATERIAL PROCESSING

The use of lasers is widespread in the material processing industry, in many applications including, welding, drilling, cutting and piercing. Different types of lasers are developed for various purposes. Commonly used types of lasers include solid-state, free electron, gas and dye lasers. (Steen & Mazumder 2010, p. 32-50.)

Laser scribing in ultrafast laser processing
Laser scribing is a commonly used process in the forming of kerfs, for example in the separation of semiconductors and ceramics. On some materials, maximum scribing speeds of several meters per second can be achieved. Applications for laser scribing can be found in multiple industries including electronics, packaging and photovoltaics industries. (Laser Scribing Eases the Further Mechanical Processing.)

Micromachining with ultrafast lasers differs significantly from working with more conventional laser processes, which utilize either continuous wave (CW) lasers or lasers with a longer microsecond scale pulse rate. The main differences lie in the material removing process. When using long-pulsed lasers, the ablation of the processed material occurs as an expulsion of melted material that is driven by the pressure of the created vapor in addition to the recoil pressure of the light. These processes are more unstable, due to the melt layer re-solidifying, resulting in changes to the geometry of the vaporized feature. The three different types of material interactions resulting from the laser processes discussed in this chapter are illustrated in figure 12. From left to right, the interactions are as follows: continuous wave (CW), nanosecond (ns), and picosecond to femtosecond (ps/fs) lazing pulses. The red areas on the arrows illustrate length of the laser pulses. The dark areas close to the surfaces indicate the size of the heat-affected zone (HAZ) and the curved blue lines illustrate the shockwave propagation resulting from the light pulses.

The removal material by a continuous wave type lase occurs mainly thru melting, thus producing a large HAZ, introducing relatively large amounts of heat to the target. The nanosecond lazing pulses create a considerably smaller HAZ, as the removal of the material occurs thru the expulsion of molten material that derives its expulsion force from the created

vapor pressure as well as the recoil pressure on the affected point. Using ultrafast pulses (ps/fs), the affected material particles are directly vaporized, removing them from the workpiece without creating of a recast layers providing for a HAZ of negligible size, resulting in highly defined and crisp features. (Lucas & Zhang 2012.)

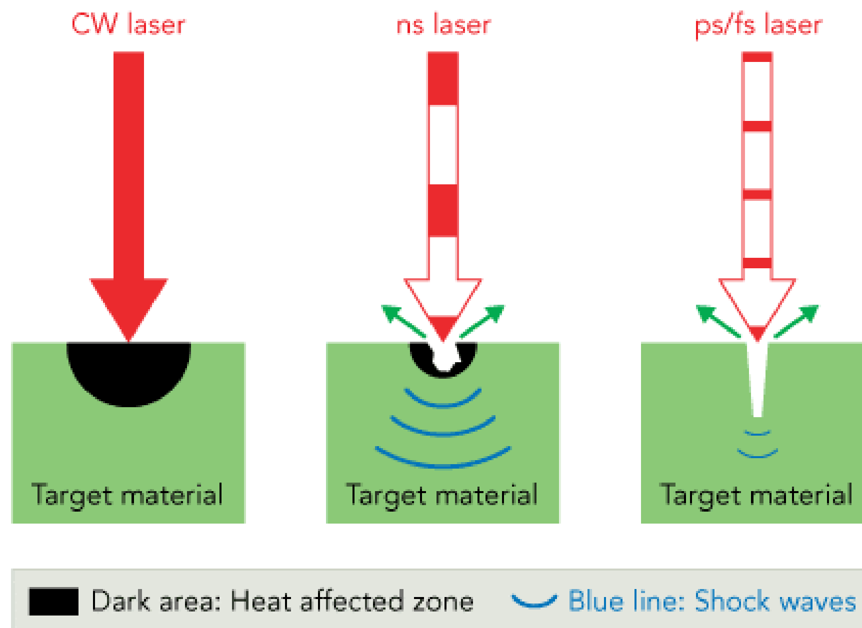

Figure 12. Laser material interaction basics for different types of lasers (Lucas & Zhang 2012).

Figure 13, shows experimental results of glass processing with a nanosecond laser in comparison with a femtosecond laser. The femtosecond laser used to produce the result pictured on the right uses a pulse duration that is more than two million times shorter. As is clear from the figure, the shorter pulse duration provides for a much cleaner and smoother hole-geometry. (Lucas & Zhang 2012.)

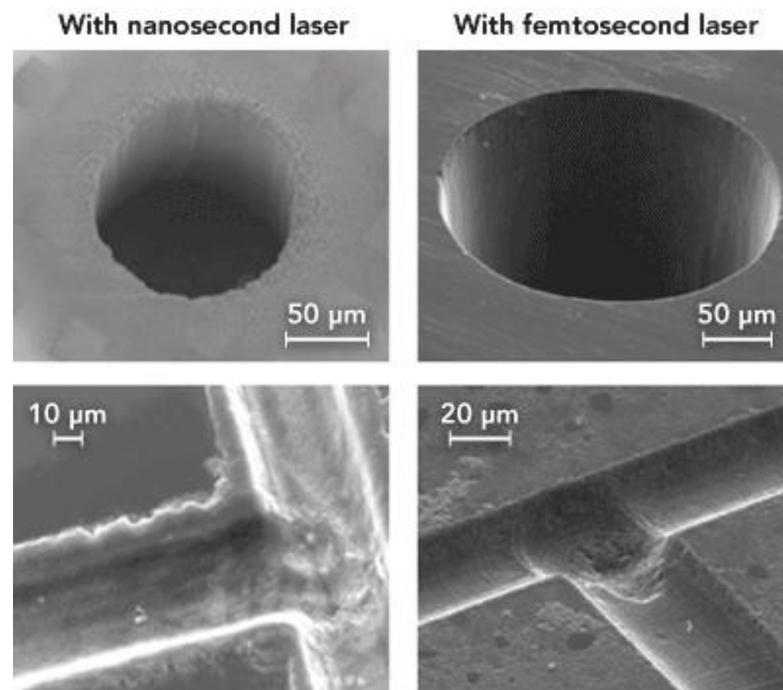

Figure 13. Laser processing examples on glass with a nanosecond laser (left-side) and with a femtosecond laser (right-side) (Lucas & Zhang 2012).

5.1 Ultrafast lasers in solar panel manufacturing applications

Copper indium gallium selenide (CIGS) is rapidly growing in popularity as a material for thin-film photovoltaics, mainly due to its good efficiency. Laser scribing of CIGS material has proven problematic. As a result of this, mechanically scribing with the use of an actively force-controlled stylus is the current industry norm for processing CIGS. But the mechanical manufacturing method has its own problems, including poor edge quality and scribing lines of irregular quality that demand significant space in between the adjacent scribes, reducing solar cell efficiency. (Rekow et al. 2010, p. 1.) Switching from mechanical scribing methods to laser scribing methods would allow for an up to four percent increase in solar cell efficiency (Eberhardt et al. 2010). The better efficiency is achieved due to the fact that an ultrashort-pulsed laser removes layer sections in between the deposition phases and creates "monolithic cell-to-cell interconnections" that result in minimal loss of productive surface-area. Lasers with an ultrashort pulse length also provide the necessary process selectivity and minimized thermal loading in the surrounding bulk of the scribed material. (Burn et al. 2012.)

6 EXISTING PHOTODIODE MONITORING APPLICATIONS FOR LASER PROCESSES

Monitoring systems are widely studied and developed for different laser processes monitoring applications. The purpose for monitoring of processes is to gather data from the process and using that information in the development of quality control methods. Plenty of monitoring applications are available for monitoring laser welding processes and in recent years, closed-loop systems are also being widely implemented. Improvements in digital information processing as well as the increased availability of quality monitoring components and technology have resulted in an increased development of systems used for monitoring lase processes. (Purtonen, Kalliosaari & Salminen 2014.)

When a real-time monitoring signal is not utilized by the system to actively control the operating parameters of the system, these types of systems are called open-loop systems. The nature of an open-loop system means that the process does not correct for deviations in its operation. The data is only collected and defects logged, and this information may be used separately to improve system operation. The demand for product quality and process reliability, without sacrificing productivity, has in recent years increased interest in closed-loop control systems and adaptive processes. Closed loop systems are developed by utilizing simple sensors, like photodiodes for example. (Purtonen et al. 2014, p. 1223.)

Photodiode monitoring has been extensively utilized in laser processes such as cutting and welding. These processes lend themselves well to monitoring due to their relatively slow speed. Laser welding in particular combines a requirement for high process quality with a slow processing speed. In addition, since the laser path is fixed in relation to the welding head, it is easier to focus monitoring sensors on the lazing event.

6.1 Laser Welding Monitor

There are plenty of technologies available for Laser Welding Monitoring (LWM). APPOLO monitoring project team had a plan to utilize and integrate a LWM system for use in the monitoring of a laser scribing process. The LWM system which was used, is a system manufactured by PRECITEC.

6.2 System description of the Laser Welding Monitor LWM

The Laser Welding Monitor LWM - system description states that, “The Laser Welding Monitor LWM is a real-time monitoring system for series production and it provides online quality-relevant information about laser welding seam”, when used in a laser welding process. Detecting variations in the appropriate weld parameters, indicating when the process has deviated from its acceptable range of operation, resulting in deviation from the weld path or a lack of effective fusion. The “finger print” of the specific welding process is acquired from reference values for produced plasma, amount vaporized metal, and the operating temperature or incoming laser radiation. The reference criteria are compared in real-time to the signals produced by the currently active process and analyzed for required corrective actions. (Laser Welding Monitor LWM - system description.)

The system is a self-sufficient real-time measurement tool for the monitoring of solid state, CO_2 and diode lasers during the process, with non-contact signal recording and calculation capability that is adaptable to the process depending on the welding progress. The LWM provides information on defects such as penetration depth, full depth, failures, seam position, porosity, spatter, etc. It enables process learning and, where possible, error correction, process improvement and adaptation over operating time.

Deviations in laser operating parameters such as lasing power, correct focal position and the adequate supply of shielding gas or its volume flow are identified, determined and analyzed. In addition to partial welding errors such as lack of fusion, component deviations like burrs on the welding joint as well as defective clamping devices are also detected. The “finger print” of the used welding process is detected thru a set of time based reference values for the back reflected plasma fume, metal fume, temperature or laser beam. While welding the signals are compared with the reference parameters. Deviations are reported to the machine in real-time.

6.3 Configuration examples

The LWM system is available in several configurations. Some of these configurations are illustrated in figure 14.

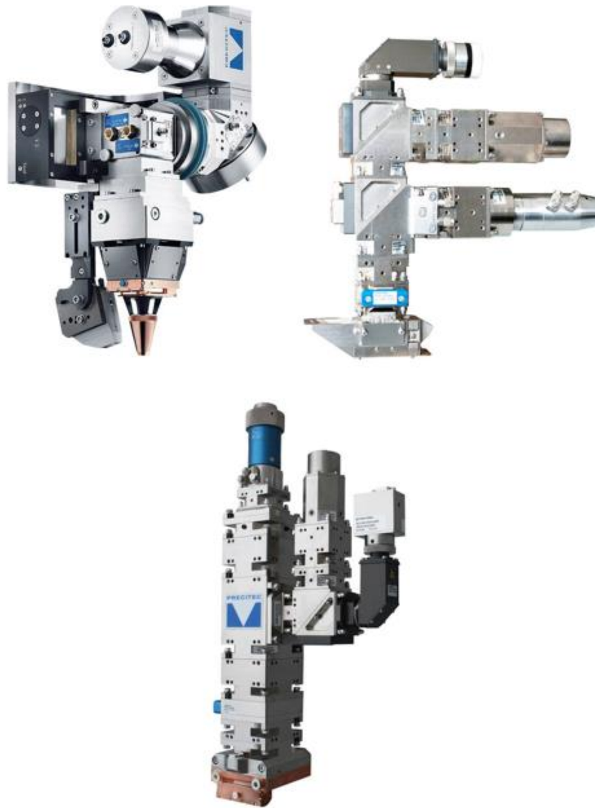

Figure 14. Examples of PRECITEC LWM configurations (Laser Welding Monitor LWM - system description).

6.4 Technical Data

LWM technical data is as below:

- The device has 16 digital inputs and 16 digital outputs
- It can contain 32 programs, and this is expandable to 128 or 256 programs
- It can contain a maximum of 8 parallel processing channels
- The maximum number of detectors is 16
- It has a maximum sampling rate of 40 kHz
- The available detectors include: laser power, temperature, plasma and back reflection

(Laser Welding Monitor LWM - system description.)

6.5 Laser Power Control

This device is designed for automatic control of the lasing power of a laser welding system during the welding process. The input is the temperature signal of an optical sensor from, e.g. the YW50 welding head. This signal is amplified in the Head Monitor HM 140 LWM or the address space layout randomizer (ASLR).

A nominal to actual value comparison in the laser power control system provides an output of DC voltage to the connected DC power control input of the laser for controlling the laser power. The actual value is provided on a second output pin also carrying DC-voltage.

A SUB-D 9 pin connector on the rear panel is for connecting the LWM to show both channels of the YW50 head on the monitor of the LWM System. The laser power control unit features are:

- 2 measuring channels
- Settings through front panel or input/output (I/O) interface on the rear panel from the programmable logic controller (PLC)
- 4 set point values (Sp1..Sp4) are programmable
- 4 programmable set point values (Sp1..Sp4); choosing via the front panel or the switch signals of the I/O's-Interface
- Set point value can be given through an analog voltage from external between 0,3 and 9,7V (Set point value extern)
- Integrated supply voltage for the up reamed preamplifier (HM 140 LWM or ASLR)
- Restricting the maximum laser power (Max Power)
- Restricting the minimum laser power (Min Power)
- Automatically setting the proportional integral derivative (PID) -parameter, depending on the delay time
- Manual dynamic setting (Dyna. PID) of these values possible

Figure 15, illustrates the laser control unit communication with the laser unit.

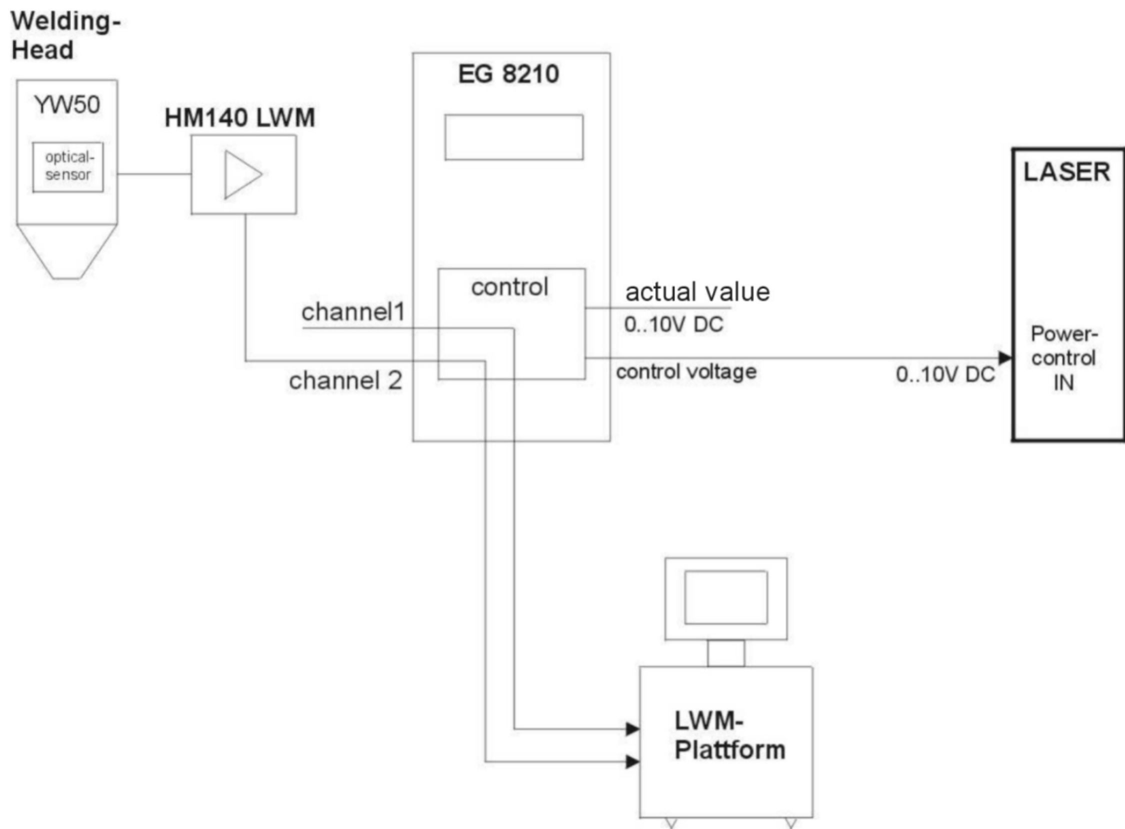

Figure 15. Laser control unit communication with the laser unit.

7 TEST SETUP

This chapter presents the equipment and testing setups utilized in this research. Specific information and component descriptions along with their use is presented in detail.

Based on the controller design principles presented in a previous section dealing with controller design, a new control system with a specific approach to controlling the scribing laser is designed for use in the APPOLO Monitoring system. Figure 16, illustrates the applied control method. In this system, the operator enters the commands using the laser human-machine interface (HMI). All the sensors are feeding their outputs to a central control unit which after analyzing the data, applies the necessary changes to the laser working parameters to minimize the process error.

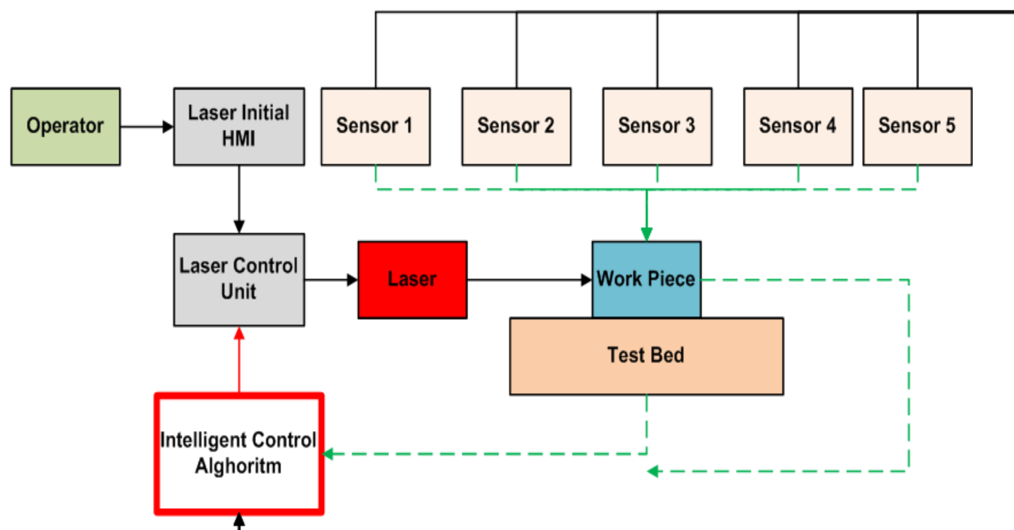

Figure 16. APPOLO controller diagram.

The entire system incorporates monitoring tools which include a spectrometer, a high-speed camera with an active illumination system, online photo diodes monitoring system and a synchronized motorized XYZ table. This thesis focuses on the photodiode component of the system.

7.1 Pulse laser

The working laser that is used for scribing in the experiments is a pulsed ytterbium fiber laser manufactured by IPG. Its average power maximum is 20 W, and typically achieves an M2 beam quality of 1.5, 1 mJ maximum pulse energy, along with a 1.6-1000 kHz repeating rate, and an incrementally variable pulse length that ranges from 4 ns to 200 ns, divided in to 8 increments. The scanning head optic utilized with the laser is a Scanlab Hurryscan 14 II with a 100 mm focal length tele-centric lens. Giving the laser a working area of 54x54 mm^2 with a minimum laser spot size of 28 µm. Actual working spot size is approximately 40 µm due to difficulties in focusing the beam with the available setup. Used laser control software is the SamLight 3.0.5 build-0582 from Scaps GmbH.

7.1.1 Optical characteristics

Table 2, provides information about the lasers optical characteristics.

Table 2. Laser optical characteristics (Specification Ytterbium Pulsed Fiber Laser YLPM-1-4x200-20-20 2009, p. 2).

N	Characteristic	Test condition	Symbol	Min	Typ	Max	Unit
1	Mode of operation			Pulsed			
2	Polarization			Random			
3	Selectable pulse durations		T1-T8	4, 8, 14, 20, 30, 50, 100,200			ns
4	Central emission wavelength	$P_{out}=P_{nom}$	λ	1055	1064	1075	nm
5	Emission bandwidth	F_{WHM}	$\Delta\lambda$		5	10	nm
6	Nominal average output power		P_{nom}	19	20	21	W
7	Output power adjustment range			10		100	%
8	Extended pulse repetition rate		RR	1.6		1000	kHz
9	Maximum pulse energy	$P_{out} = P_{nom}$, $T=T_8$ (200ns)			1		mJ
10	Maximum peak power				15		kW
11	Laser switching ON/OFF time				2	3	μs
12	Long-term average power instability	$P_{out} = P_{nom}$ over 5 hrs			2	5	%

7.1.2 Optical Output

Table 3, provides information about the laser optical output.

Table 3. Laser optical output (Specification Ytterbium Pulsed Fiber Laser YLPM-1-4x200-20-20 2009, p. 2).

N	Characteristic	Test condition	Min	Type	Max	Unit
1	Protection cable type		metal shielded /PVC coated			
2	Delivery cable diameter		6		7	mm
3	Output fiber cable length			2		m
4	Output beam diameter	l/e^2 1evel	6			mm
5	Beam quality M^2			1.5	2.0	

7.1.3 Electrical Characteristics

Table 4 provides information about the laser optical output.

Table 4. Laser electrical characteristics (Specification Ytterbium Pulsed Fiber Laser YLPM-1-4x200-20-20 2009, p. 3).

N	Characteristic	Test condition	Min	Type	Max	Unit
1	Supply voltage		23	24	25	VDC
2	Current consumption				6	A

7.1.4 General Characteristics

Table 5 provides general information about the laser.

Table 5. Laser general characteristics (Specification Ytterbium Pulsed Fiber Laser YLPM-1-4x200-20-20 2009, p. 3).

N	Characteristic	Min	Type	Max	Unit
1	Environment temperature range ■ 100% emission time ■ 50% emission time	0		+40 +45	°C
2	Warm-up time to start of operation			10	s
3	Humidity (non-condensed environment)	10		95	%
4	Laser module dimensions	233 x 59 x 292			

7.1.5 Control Interfaces, configuration and operating modes

The control interface of the laser uses a DB-25 connector-plug for connecting the digital signals. Also there is a RS-232C interface available including a DB·9 connector-plug. Standard laser configuration and options as listed in Specification Ytterbium Pulsed Fiber Laser YLPM-1-4x200-20-20 (2009) are:

"Standard laser configuration includes:

- Bitstream 1 (BS1) mode including high contrast (HC)
- Extended pulse repetition rate
- Output isolator

Options:

- Guide laser (red aiming diode)
- Output beam diameter alteration
- Delivery fiber length alteration
- Power supply 100/240 AC autoranging
- USB Remote control, laboratory grade (including PC software)"

Table 6, shows the compatible combinations of modes which are available in the laser.

Table 6. Laser operating modes (Interface Specification YLP series Ytterbium Pulsed Fiber Lasers Interfaces "type D" and "type D1" 2009, p. 13).

Option/ Mode	Description
RS-232	RS-232 control interface
HC	High Contrast
Ext. PRR	Extended Pulse Repetition Rate
BS	Bit stream mode
BS1	Bit stream 1 mode
Adj. Pulse	Adjustable Pulse mode
Jump PRR	Jump Pulse Repetition Rate

The "RS-232C" allows for the control of the laser using a RS-232 port. "HC high-contrast" option can make sure that power leakage is kept minimal if the modulation signal of the emissions is kept at a low level and the signal enabling energy emission is set high. In lasers that aren't provided with this possibility, some power leakage will occur from the output, the magnitude of which is dependent on the model of the particular laser in question. If the BS1 operation mode is set to active, a continuous wave emission of residual output power can occur. "Ext. PRR" Extended Pulse Repetition Rate (PRR) function allows for operation with the PRR set to a smaller value than what the nominal. There is proportionally lover average power output available when using the PRR at a lower setting. This way the energy of the pulses can be kept at a constant level. The "BS" bit stream mode of operation permits the modulating of each individual pulse. When operating the laser at a set PRR, the electromagnetic (EM) signal can be utilized for masking. If the EM is high the pulses are allowed to emit at the pulse synchronization signal. If the EM is low there will be no pulse emitted. A constant time-shift exists, which is usually 256f,1s, but this is dependent on the particular model. This time shift in between the first of the rising edges of the PRR signal, and after the rising of the EM, and the emission of the optical pulses train. The HC option is invariably included in the options, if the BS option has been included. One example of the aforementioned control diagram is illustrated in figure 17. (Interface Specification YLP series Ytterbium Pulsed Fiber Lasers Interfaces "type D" and "type D1" 2009.)

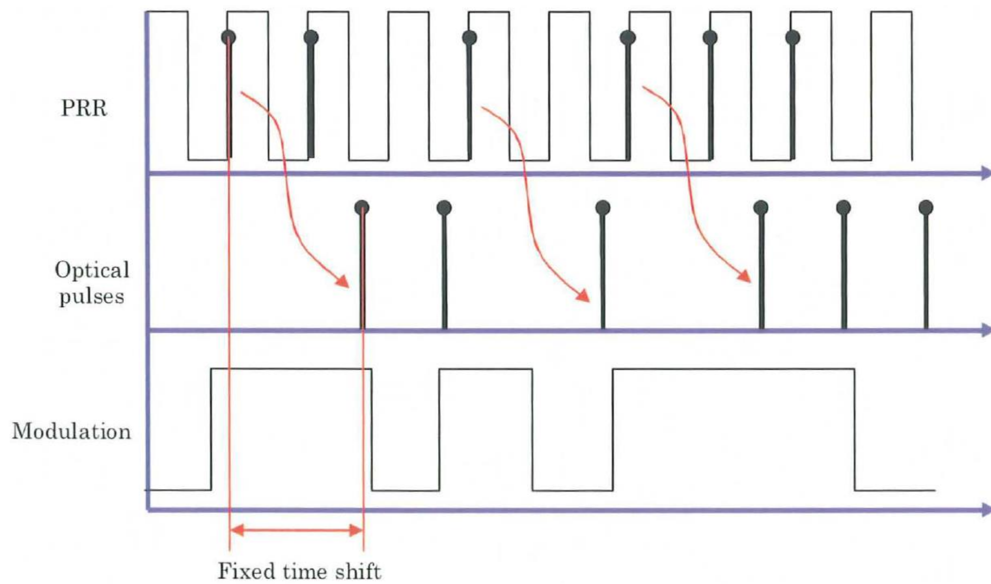

Figure 17. An example of a control diagram (Interface Specification YLP series Ytterbium Pulsed Fiber Lasers Interfaces “type D” and “type D1” 2009, p. 14).

The “BS1” bit stream 1, mode of operation permits the modulating of each individual pulse. The EM signal can be used for masking when the PRR is set to constant value. The pulse synchronization signal will initiate emission if the EM signal is at a high level. If EM is low there will be no emission of pulses. The small delay time of usually less than 2~lS, that varies by model, existing in between the rising edge of PRR and the peaking of the EM signal and the emission of the optical pulse. This HC option is invariably delivered, when the BS1 option is included. An illustration of a controlling diagram sample is shown below in figure 18. The BS1 option, is not like the BS option, it needs the laser to be prepared to begin emission instantaneously. The leakage resulting from this are minimal amounts of CW power in the EE ON and EM OFF states. Options BS and BS1 are ideally suited for creating raster markings. (Interface Specification YLP series Ytterbium Pulsed Fiber Lasers Interfaces “type D” and “type D1” 2009.)

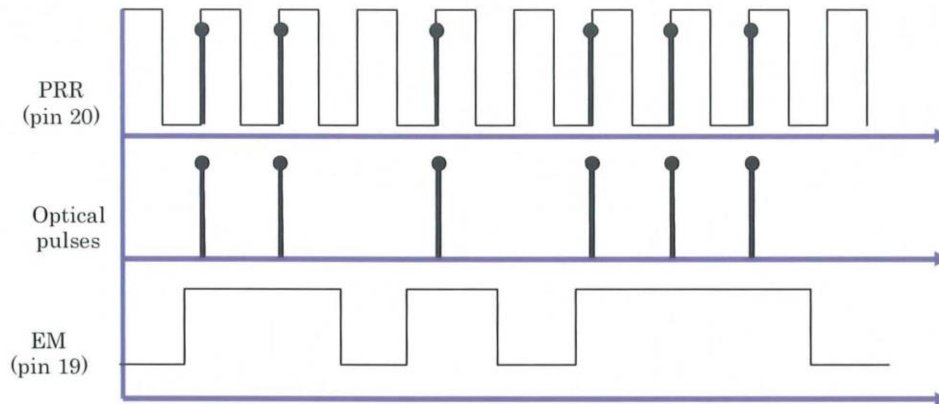

Figure 18. An example of a control diagram for BS1 (Interface Specification YLP series Ytterbium Pulsed Fiber Lasers Interfaces "type D" and "type D1" 2009, p. 15).

The "Adj. Pulse" Adjustable pulse duration option permits the choosing of the form and length of the optical pulses from a preexisting list of discrete options. This set of preexisting shapes for the optical pulses is determined by the devices operating specifications and is calibrated in factory after assembly. (Interface Specification YLP series Ytterbium Pulsed Fiber Lasers Interfaces "type D" and "type D1" 2009.)

7.1.6 RS-232C electrical connector

The RS-232C electrical connector has a DB9 "male" plug-type. The RS-232C interfaces with a connection that is galvanicaly isolated from the digital interface as well as the internal laser grounding. These features aide in avoiding any major problems that arise from current loops produced in complicated interfacing interconnections. Pin assignments in the interface conform to the standards for communicating with PC COM ports. (Interface Specification YLP series Ytterbium Pulsed Fiber Lasers Interfaces "type D" and "type D1" 2009.)

7.1.7 Laser Control Software

The laser control software is SAMLight which is a product of SCAPS GmbH. SCAPS is a leading software manufacturer for controlling scanner and laser systems. SAMLight covers all of the features for the various kinds of applications that use a galvanometer scanner in combination with a laser bringing light to the material. SAMLight is based on SCAPS SAM technology and provides the functionality for many industrial applications as well as for research purposes.

7.2 Scan Head

The scanner head is manufactured by SCANLAB. The model of the scanner head is HurrySCAN II. This compact scan head is able to provide an optimal solution for industrial level material laser processing applications. These scan heads have inter connectable mechanics and electrical systems, with aperture sizes that range from 7 mm to 30 mm and multiple levels of dynamic performance. With excellent stability in long term use and very minimal drifting that are made possible by integral temperature stabilizing features. A smaller working aperture system combines great speed with extraordinary precision in an optimal package. Marking speed of these devices exceeds 1000 characters per second without difficulty. Figure 19, illustrates a HurrySCAN scanner head. (SCANLAB website.)

Figure 19. A HurrySCAN scanner head (SCANLAB website).

Typical applications of this scanner head are: Micro processing of material, Surface marking, Micro-structuring, Rapid manufacturing, three dimensional applications. Figure 20, shows the layout of the scanner head and figure 21, illustrates HurrySCAN scanner head scheme of operation. (SCANLAB website.)

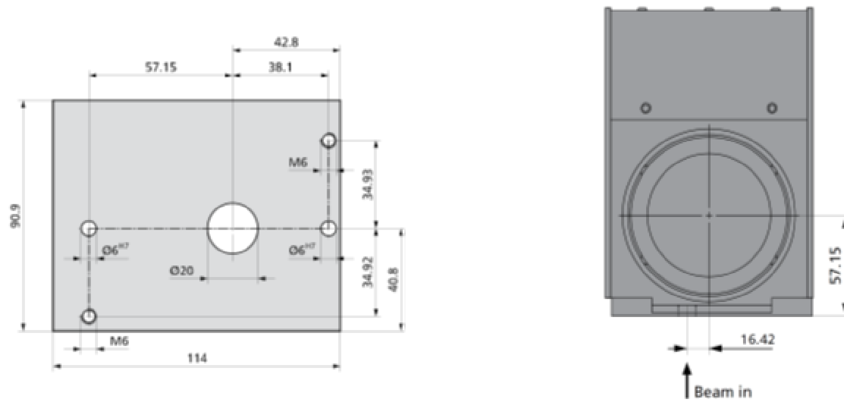

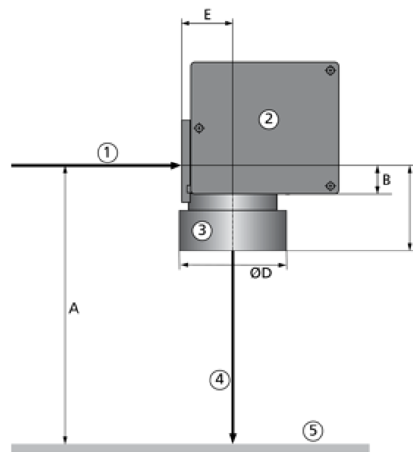

Figure 20. The layout of the scan head (SCANLAB website).

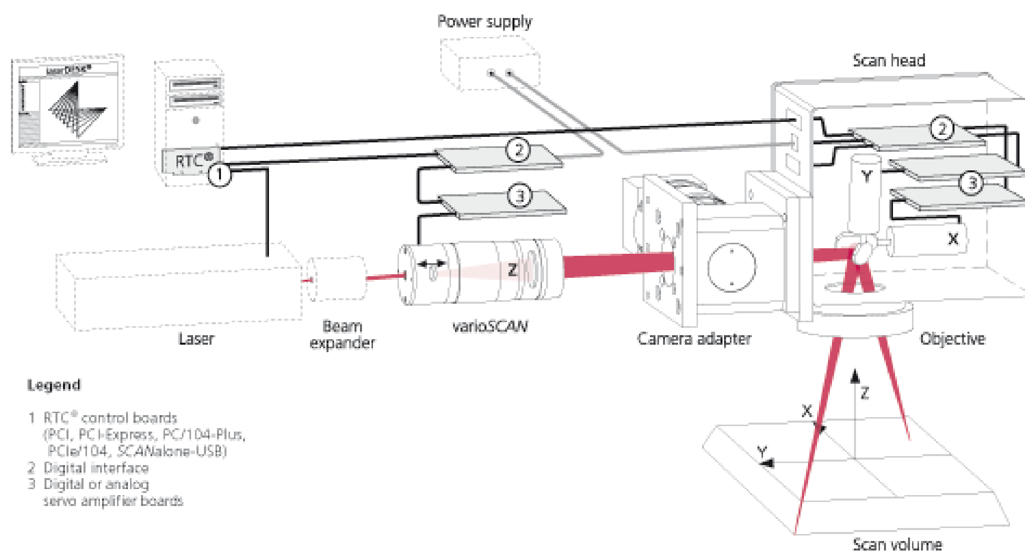

Figure 21. HurrySCAN scanner head scheme of operation (SCANLAB website).

The scan head is equipped with standard digital interfaces which are controlled thru SCANLAB's real time control (RTC) board. Table 7, lists HurrySCAN II technical information. (SCANLAB website.)

Table 7. Laser scan head operating modes (SCANLAB website).

Parameter			Value
Aperture			14 mm
Tracking error			0.24 ms
Step response time	**1% of full scale**		0.40 ms
	10% of full scale		1.60 ms
Typical speeds	**Marking speed**		1.5 m/s
	Positioning speed		7.0 m/s
	Writing speed	**Good quality**	500 cps
		High quality	340 cps
Long-term drift (8-h-drift)			< 0.6 mrad
Optical performance	**Typical scan angle of scanner 1**		± 0.35 rad
	Typical scan angle of scanner 1		± 0.35 rad
	Typical field size - ellipse		-
	Typical field size - square		90×90 mm^2
	Nonlinearity		<3.5 mrad /44°
Weight (without objective)			approx. 3 kg

7.2.1 Control Boards

SCANLAB's RTC control board is PC platform solution for the control of a laser scan system. Software commands allow these RTC boards to have completely synchronized control over the scanning systems and the connected lasers in a real time. In an RTC package, the following features are included:

- Imaging field corrections two and three dimensional space
- Evaluation of status signals
- On the fly processing for moving objects
- Control of a triple axis scanning system
- Functionality for the simultaneous control of two separate scan systems

- Data interface with optic fiber connection

SCANLAB's RTC PC interfacing boards provide synchronized, controlling of scanning systems and lasers in real time in a package that is resistant to outside interference. Figure 22, shows the RTC board. (SCANLAB website.)

Figure 22. Scan head RTC boards (SCANLAB website).

The RTC provides signal processing at a high level of performance and the dynamic link library (DLL) included in the supply simplifies programming in a Windows platform. Alternative software offerings are also available from several third-party suppliers, which offer a diverse selection standard applications. (SCANLAB website.)

The loading of the software's instructions alternates between the RTC's two list buffers that are then processed in the digital signal processor (DSP), and put out as 16-bit controlling signals once every in 10 µs through to the scanning system. The RTC's internal processor performs an automated set of crucial actions such as adjusting the micro-vectors as well as correcting errors in the imaging field. Controlling of the laser is conducted in synchronous operation with the movement of the scanner. Multiple laser control signals for vector or bitmap processing available for programming. Specifications of RTC are:

- Peripheral component interconnect (PCI) bus interface
- Selectable laser modes
- 16-bit positioning resolution (e.g. YAG modes, C02 mode, polarity)

- 10 µs output period
- Two 10-bit resolution analog outputs along with one 8-bit digital output
- A maximum of 8 RTC19 boards integrated to 1 PC (only 32-Bit DLL available)
- Outputs for controlling a single scanning head with a single laser
- One digital input and one digital output for the control of external components, both 16-bits
- Triple axis control of scanning system
- Data transfer thru an interface with an optical fiber connection
- On the fly processing for working with moving objects
- Ability to simultaneously control 2 scanning systems
- 16-bit digital input, and similar output with four opto-decoupled bits
- 4 analog inputs and outputs, with a 10-bit resolution each

(SCANLAB website.)

7.3 Camera Adapter

A Scanlab camera adapter, is installed on the scan head to allow for a viewing area which follows the scribing laser beam for continuous monitoring of the area which is being processed by the laser. The adapter offers effortless attachment into new and previously existing laser systems. The mechanical interface of the adapter facilitates simple and easy mounting to the scanning head and again to lasers attachment flange. The attachment configuration permits attachment in four possible orientations of the adapter relative to the observer. (SCANLAB website.)

In order to enable the monitoring of the entire working surface, incoming light that arrives from the work piece is decoupled with the use of the adapter beam splitter and redirected through the adapter aperture in to which ever sensor is connected. On the other hand, the scribing laser itself passes essentially un-attenuated thru the beam splitter to the scanning system. Multiple optical configurations are offered for a multitude of usable wavelengths. Figure 23, illustrates the scan head monitoring adapter.

A picture of the camera adapter is presented in figure 8 and the technical information of the adapter is presented in table 8. (SCANLAB website.)

Figure 23. The scan head monitoring camera adapter (SCANLAB website).

Table 8. Technical information of the camera adapter (SCANLAB website).

Diameter of entering beam	Max 30 mm
Connection type for camera Maximum chip size of camera	C-Mount 2/3“
Weight	ap. 1.6 kg
Operation temperature	25 °C ± 10 °C

7.3.1 Installation

The mounting of camera adapter is made in the space between the scanning head’s beam entry hole and the mounting flange of the laser. The boreholes located at the camera adapter beam entry and exiting sides are fully compatible with the complimentary apertures on the HurrySCAN II scanning head, made by SCANLAB. The housing for the beam splitters is adjustable for obtaining the optimal orientation of sensor unit in relation to the objective unit. The orientation options include up, down or on either side of the scanning head. Drawings for the camera adapter are shown in appendix I. (SCANLAB website.)

7.3.2 Operating principle

This camera adapter component allows for observing the working area of the scanning head. A dichroic beam splitting element contained in the beam splitter's housing decouples the light coming in thru the lasing aperture from the illuminated working surface. This light which arrives thru the scanning head beam window from the scanning head's objective and reflected by the scanning head mirror system. Part of the illumination entering the adapter thru the scan head is split into a path which is perpendicular the path of the entering beam, and is then directed towards the sensor attachment port (SCANLAB website). The scribing laser beam, is allowed to pass through the beam splitters dichroic reflector practically unaffected. The decoupled light is directed through the camera attachment port to whatever sensor is attached to the adapter. Figure 24, illustrates the camera adapter's principle of operation. Table 9, presents the specifications of the monitoring adapter unit.

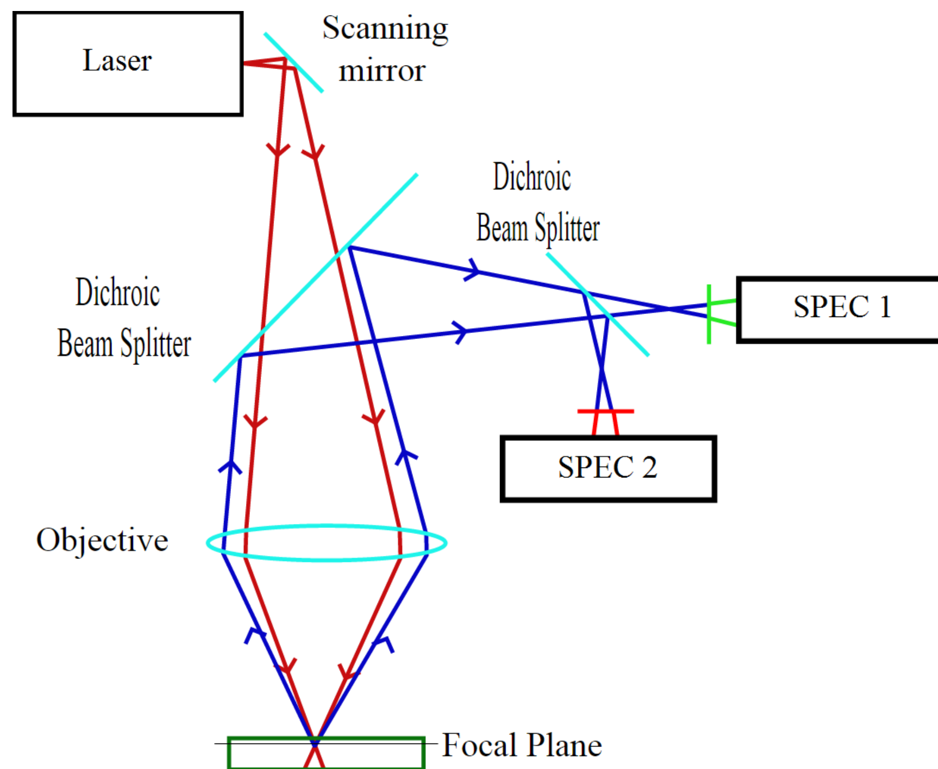

Figure 24. The principle of the camera adapter operation (SCANLAB website).

Table 9. The specifications of the camera adapter unit (SCANLAB website).

Typical Optical Configurations with Scan Head

Laser wavelength	1064 nm	532 nm	355 nm	266 nm
Observation wavelength	880 nm	635 nm	635 nm	635 nm
Scan head aperture	14 mm	10 mm	10 mm	10 mm
Scan head mirror coating (1)	1064 nm + 880 nm	532 nm + 635 nm	355 nm + 635 nm	266 nm + 635 nm
Flat field objective	163 mm	160 mm	100 mm	103 mm
Processing field size	110 x 110 mm^2	110 x 110 mm^2	50 x 50 mm^2	50 x 50 mm^2
Beam splitter				
Laser wavelength	1030 nm - 1110 nm	488 nm - 532 nm	350 nm - 360 nm	257 nm - 266 nm
Range for observation wavelength(1)	450 nm - 900 nm	615 nm - 900 nm	510 nm - 680 nm	630 nm - 670 nm

7.4 Industrial computer (PXI-system)

PCI eXtension for Instrumentation (PXI) system is a PC-based control and computation platform for measuring and automating process systems and applications. A PXI combines PCI (Peripheral Component Interconnect) electrical bus features with the modularly customizable, Eurocard packages of Compact PCIs and then includes special customizing bus sets and crucial software features. The PXI deployment platform is used for applications such as testing manufacturing processes, aerospace and military plications, monitoring of industrial machines, automotive industry applications, as well as various testing applications in several industries.

The computer of the PXI Data acquisition system assembled for the experiments is shown in figure 25. The whole system consists of NI BNC-2120 shielded connector block, NI PXIe-6363 X Series Data Acquisition card and NI PXIe-8880 Real-Time Controller Module. These modules are assembled using a NI PXIe-1071 Express chassis. The basic parts and module expansion principle are shown in figure 26. The different modules are presented in the following sections.

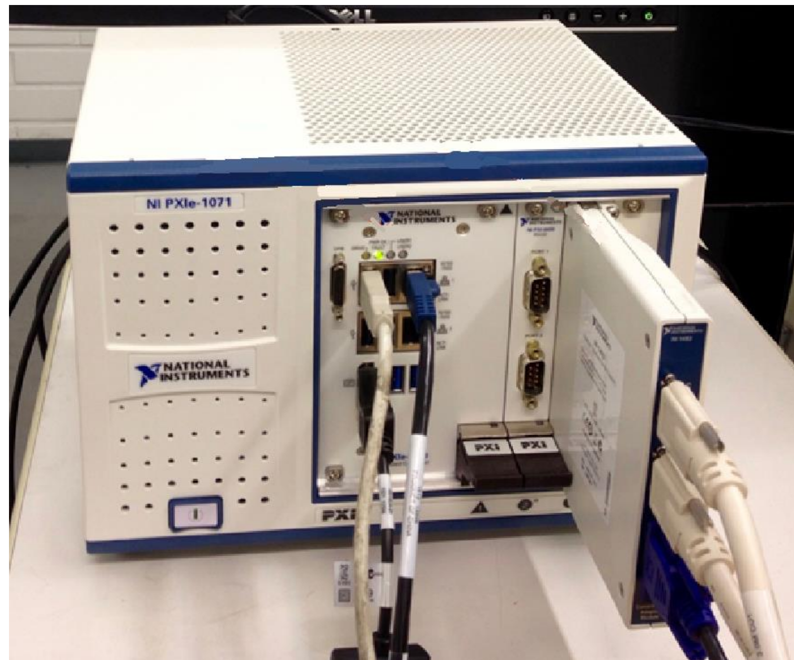

Figure 25. The PXI system main unit, PXIe-1071 Express chassis with a PXIe-8880 Real-Time Controller Module.

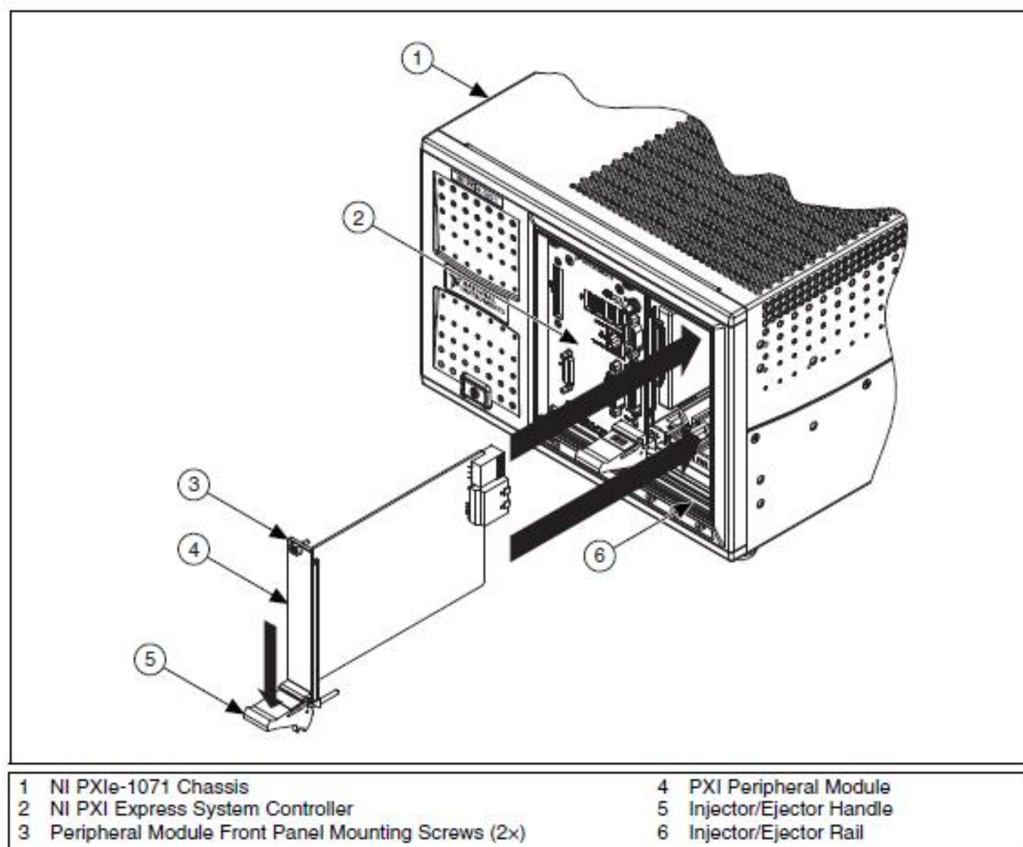

Figure 26. PXI System (NI PXIe-1071 User Manual 2013, p.2-11).

7.4.1 PXIe Real Time module

The “NI PXIe-8880 embedded controller” provides the processing capability of an Intel “Xeon workstation” Central Processing Unit for testing and validation of engineering an industrial applications. This multiple core package computing power provided by the Intel Xeon the PCI Express Generation 3 technology provides double the bandwidth and double the performance of the PCI Express Generation 2 technology, and its 8 cores give twice the processing capacity of a quadruple core central processing unit (CPU) with low latency. That makes it suitable for high-speed real time process monitoring applications. (NI PXIe-8880 User Manual 2015.)

The NI PXIe-8880:

- Intel Xeon E5-2618L
- 3.4 GHz per core
- Octa-Core (8 core processor)
- “16 hyper threaded virtual cores”
- “Triple channel 1866 MHz DDR4 memory”

(NI PXIe-8880 User Manual 2015.)

7.4.2 NI BNC-2120 connector block

NI BNC-2120 shielded connector block is used for connecting sensor inputs to the control system using Bayonet Neill-Concelman connectors (BNC). The connector block is connected to the NI PXIe-6363 data acquisition (DAQ) card which is presented in a following section, and is installed as a part of the control system. The BNC-2120 connector block is shown in figure 27, and the connector block front panel in figure 28.

Figure 27. NI BNC-2120 shielded connector block (NI BNC-2120).

The following list describing the technical specifications of the NI BNC-2120 shielded connector block is taken from the BNC-2120 Installation Guide. The physical, operational and environmental characteristics and limitations of the BNC-2120 product as they are listed on pages 14–17 of the BNC-2120 Installation Guide (2012) are:

“**Analog Input**

Number of channels (default) ....8 differential

Field connections (default) ....8 BNC connectors

Protection ....No additional protection provided. Consult your DAQ device specifications.

Optional inputs

AI 0 ....Temperature sensor

AI 1 ....Thermocouple

AI 3, AI 11 ....Resistor measurement (requires RSE configuration)

Optional connections

Thermocouple...Uncompensated miniatureconnector, mates with 2-prong miniature or subminiature connector

Resistor ....2 screw terminals

Resistor measurement range............................ 100 Ω to 1 MΩ

Resistor measurement error .... ≤5%

Screw terminals .... 4 positions, 28–16 AWG wire

Switches

Floating source/grounded source 8

BNC/temperature reference IC 1

BNC/thermocouple connector 1

BNC/resistor screw terminals 1

Analog Output

Field connection .... 2 BNC connectors

Digital Input/Output

Screw terminals .... 9 positions, 28–16 AWG wire

LED state indicators .... 8, 1 each for lines P0.<0..7>

Protection (DC max V)

Powered off... ±5.5 V

Powered on .... +10/–5 V

Drive

Vol .... 0.6 V, 8 mA

1.6 V, 24 mA

Voh.. 4.4 V, 8 mA

4 V, 13mA

Function Generator

Square wave...TTL-compatible

Frequency range .... 100 Hz to 1 MHz

Frequency adjust...................................... Through the Frequency Adjust knob

Rise time.. 2 ns

Fall time... 2 ns

Sine/triangle wave

Frequency range .... 100 Hz to 1 MHz

Frequency adjust...................................... Through the Frequency Adjust knob

Amplitude range .... 200 mVp-p to 4.8 Vp-p

Amplitude adjust...................................... Through the Amplitude Adjust knob

Output impedance.................................... 453 Ω (sine/triangle wave)

50 Ω (square wave)

Timing Input/Output

Screw terminals..14 positions, 28–16 AWG wire

BNC connector ....1, for PFI 0/AI START TRIG

Protection (DC max V)

Powered off...±1.7 V

Powered on ....+6.7/–1.7 V

Quadrature Encoder

Screw terminals..2

Output signals

PULSES..96 pulses/revolution

UP/DN ....High for clockwise rotation,
low for counterclockwise rotation

Pulse width...1 μs

Power Requirement

+5 VDC (±5%)..200 mA, sourced from the
multifunction DAQ device

Power available at +5 V screw terminal ....Multifunction DAQ device power,
less power consumed at +5 VDC
(±5%)

Physical

Dimensions ....26.7 cm × 11.2 cm × 5.97 cm
(10.5 in. × 4.41 in. × 2.35 in.)

Weight ....1,040 g (2 lb 4.7 oz)

I/O connector .... 68-pin male SCSI-II type

BNC connectors.. 15

Screw terminal plugs 31

Environment

Operating temperature .... 0 to 50 °C

Storage temperature .... –55 to 125 °C

Relative humidity .... 5 to 90%, noncondensing

Pollution Degree 2

Maximum altitude.. 2,000 m

Indoor use only”

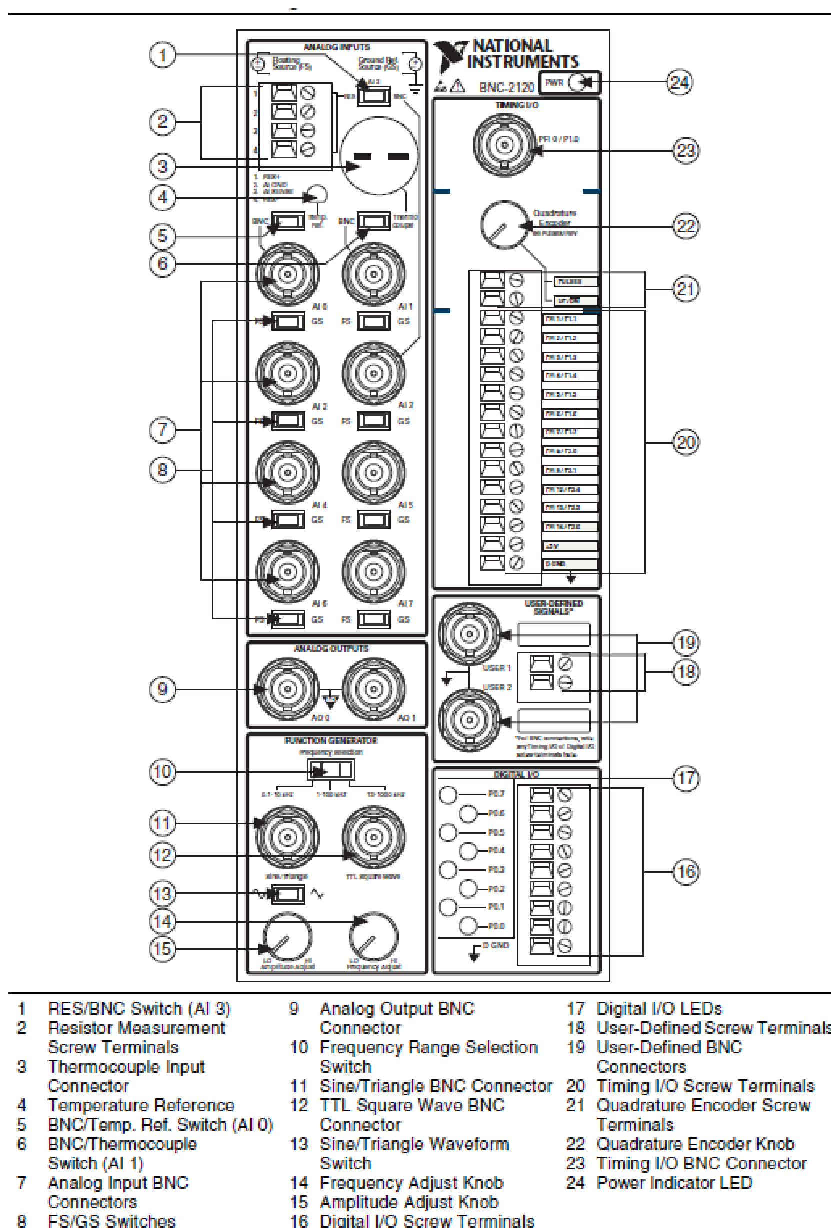

Figure 28. NI BNC-2120 shielded connector block front panel (BNC-2120 Installation Guide 2012, p.3).

7.4.3 NI PXIe-6363 DAQ card

The NI PXIe-6363 X Series Data Acquisition card is used to receive and collect the input data from the NI BNC-2120 shielded connector block, which is presented in the previous section. The PXIe-6363 Data Acquisition card is shown in figure 29.

Figure 29. NI PXIe-6363 DAQ card (PXIe-6363).

The following information is based on information gathered from NI PXIe-6363 Device Specifications document. Along with other documentation included in the device delivery.

The NI PXIe-6363:

- Multifunction DAQ
- PXI Express Bus Type

Analog Inputs

- 32 Single-Ended Channels
- 16 Differential Channels
- 16 bit Analog Input Resolution
- -10 V – 10V Maximum Voltage range, with 1.66 mV Accuracy
- -0.1 V – 0.1 V Minimum Voltage range, with 33 µV Accuracy

Analog Outputs

- 4 Channels
- 16 bit resolution
- -10 V – 10V Maximum Voltage range, with 1.89 mV Accuracy
- -5 V – 5 V Minimum Voltage range, with 935S µV Accuracy
- 2.86 MS/s Update Rate

Digital I/O

- 48 Bidirectional Channels

Physical Specifications

- Length: 162.56 mm
- Width: 20.02 mm
- Height: 100 mm
- 68-pin VHDCI female I/O Connector

(NI PXIe-6363 Device Specifications 2015.)

7.4.4 1103P Helium Neon Monitoring laser

The 1103P Helium Neon Laser from JDS Uniphase, is the laser used in this research to externally illuminate the scribe in order to provide an input for the photodiode sensor. The laser head is shown in figure 30.

Figure 30. 1103P Helium Neon Laser (Helium-Neon Laser Heads 1100 Series 2005, p. 1).

The technical information of the 1103P Helium Neon Laser head is presented in the technical specification of the product, in tables 10 and 11. These tables list the operating parameters for all of the laser heads in the JDS 1100 product range, but the 1103P type is highlighted with the squares.

Table 10. Technical specification for JDS Uniphase 1100 Series Helium Neon Laser Heads part 1/2. The 1103/P type used in these experiments is highlighted with the square. (Helium-Neon Laser Heads 1100 Series 2005 p.3).

Parameter	1101/P	1103/P	1107/P	1108/P	1122/P	1125/P	1135/P	1137/P	1144/P	1145/P	Unit
Optical											
Min. output power (TEM_{00})	1.5	2.0	0.8	0.5	2.0	5.0	10.0	7.0	15.0	22.5/21.0	mW
Wavelength	632.8	632.8	632.8	632.8	632.8	632.8	632.8	632.8	632.8	632.8	nm
Mode purity (TEM_{00})	>95	>95	>95	>95	>95	>95	>95	>95	>95	>95	%
Beam diameter (I/e2 points, ±3%, TEM_{00})	0.63	0.63	0.48	0.48	0.63	0.81	0.68	0.81	0.70	0.70	mm
Beam divergence (TEM_{00}, ±3%, mrad- full angle)	1.3	1.3	1.7	1.8	1.3	1.0	1.2	1.0	1.15	1.15	mrad
Polarization ratio (minimum, P versions)	N/A /500:1	N/A /500:1	N/A /500:1	N/A /500:1	N/A /500:1	N/A /500:1	N/A /500:1	N/A /500:1	N/A /500:1	N/A /500:1	-
Longitudinal mode spacing (nominal)	730	730	1090	1090	730	435	320	435	257	257	MHz
Maximum noise (rms, 30 Hz to 10 MHz)	0.1	0.1	0.1	0.1	0.1	0.2	1.0	0.2	0.5	0.5	%
Max. drift (mean power measured over 8 hours)	±2.5	±2.5	±2.5	±2.5	±2.5	±2.5	±3.0	±2.5	±2.0	±2.0	%
Max. mode sweeping contribution	3	3	10	20	3	2	2	2	1	1	%
Max. warm-up time (minutes to 95% power)	10	10	10	10	10	10	15	10	20	20	min.
Beam pointing stability (from cold start, 25 °C)	N/A	N/A	N/A	N/A	<0.10	<0.10	<0.10	<0.10	<0.20	<0.20	mrad
Beam pointing stability (after 15 minutes warm-up)	N/A	N/A	N/A	N/A	<0.10	<0.10	<0.02	<0.02	<0.03	<0.03	mrad
Operating voltage (V DC ±100)	1700	1700	1250	1250	1800	2300	3100	2300	3800	3800	V DC
Operating current (±0.1 mA)	4.9	4.9	4.0	4.0	6.5	6.0	6.5	6.0	6.5	6.5	mA
Dimensions											
L-overall length	9.50	9.50	7.00	7.00	10.71	15.79	19.13	15.79	25.00	25.00	inches
D-mounting diameter (±0.005 inches)	1.245	1.245	1.245	1.245	1.740	1.740	1.740	1.740	1.740	1.740	inches
B-distance: cable end to mounting surface	1.00	1.00	0.75	0.75	1.50	3.00	4.00	3.00	5.00	5.00	inches
A-distance: output end to mounting surface	0.75	0.75	0.50	0.50	1.50	3.00	4.00	3.00	5.00	5.00	inches
CDRH class (head & 1200 Series power supply)	IIIa	IIIa	IIIa	II	IIIa	IIIb	IIIb	IIIb	IIIb	IIIb	-

Table 11. Technical specification for JDS Uniphase 1100 Series Helium Neon Laser Heads part 2/2. The 1103/P type used in these experiments is highlighted with the square. (Helium-Neon Laser Heads 1100 Series 2005 p.4).

Parameter	1101/P 1103/P 1107/P 1108/P 1122/P 1125/P 1135/P 1137/P 1144/P 1145/P
General	
Maximum starting voltage	10 kV DC
Mode purity	>95%
Storage lifetime	Indefinite (hard-sealed)
Static alignment	Center to outer cylinder within ±0.01 inch. Parallel to outer cylinder within ±1 mR.
Environmental	
Temperature	-40 to 70 °C (operating), -40 to 150 °C (non-operating)
Atitude	0 to 10,000 feet (operating), 0 to 70,000 feet (non-operating)
Relative humidity (no condensation)	0 to 100%
Shock	25 g for 11 ms, 100 g for 1 ms
Physical	
Shipping weight	5 lb. (1100 Series heads); 10 lb. (1100 Series head and 1200 Series power supply)

7.5 LabVIEW System Design Software

The “Laboratory Virtual Instrument Engineering Workbench” referred to as LabVIEW, is an application developing software environment for creating custom applications that can interact with real-world input data or signals for use in different scientific fields. It differs in principle from the standard C-code and Java application developing environments in that, where these traditional programming systems use text-based languages in creating lines of code, LabVIEW relies on a graphic programming language that is called “G” to create and refine programs in a visual user interface. This makes it easier to use for developers who are not specialized in programming. (LabVIEW.)

A typical LabVIEW program involves one or several virtual instruments VIs for short. The appearance and operation of the virtual instruments is designed to imitate actual physical instruments. VIs consists of a block diagram and a “front panel”, where the block diagram functions as the main code for the VIs, as a sort of virtual internal wiring, and the front panel acts as the user interface of a VI with interactive features. The front panel meant to simulate a front operating panel on a real physical instrument or other device. It can be customized with knobs, switches, buttons, displays, and many other interactive devices, which are used as inputs and indicators. (LabVIEW.)

8 EXPERIMENTS

Several experiments were conducted using photodiodes, in order to determine the possibilities and problems involved in using commercial photodiodes for monitoring. The specific fields of interest included: optimal solution for tracing the scribing path, specular versus diffuse reflection of monitoring beam and the ability to distinguish between different material layers. It was important to test witch form of reflection gave the best contrast between the scribed and the intact surface. Also whether or not the different layers of an applicable target material, such as CIGS, had enough difference in reflectivity to be distinguished from each other. The way that the scribing laser moves during the process also presents difficulties in following the scribe path. All of these experiments are presented in greater detail below. The average scribe with used in these experiments was approximately 50 µm. Figure 31, shows an example of testing setup used in the experiments.

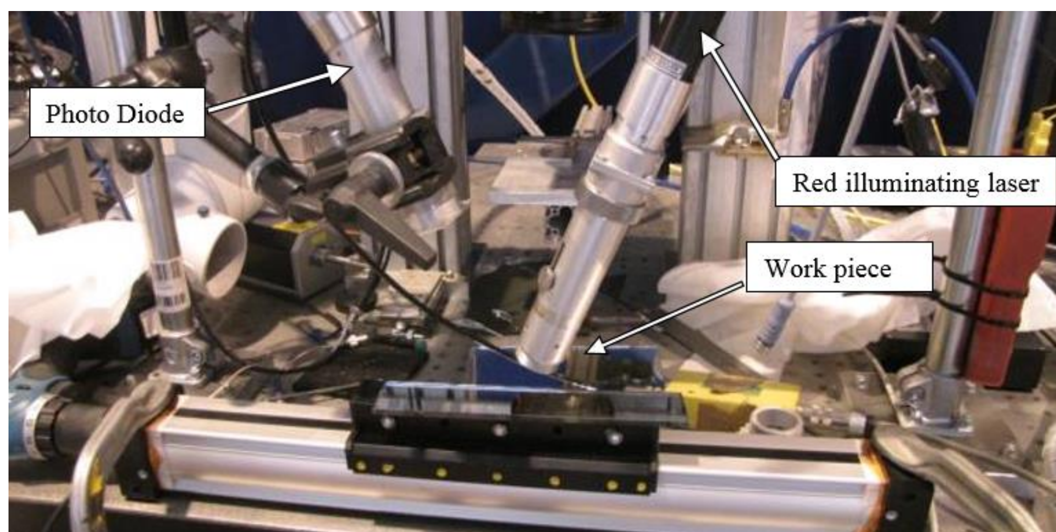

Figure 31. Example of a monitoring test setup.

8.1 Specular and Diffuse Reflection

The difference between specular and diffuse reflection, as seen in figure 32, is that specular reflection is the portion of light that is directly reflected in an angle that is equal to the angle of incidence of the incoming beam. Diffuse reflection however is the portion of light that is scattered in all other directions, due to irregularities in the surface that prevent perfect reflection.

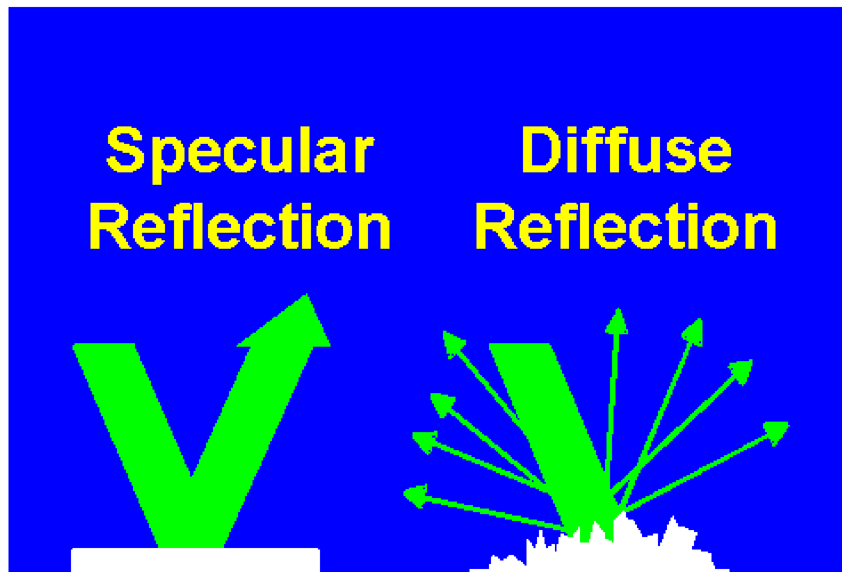

Figure 32. Specular (left) and diffuse (right) reflection.

Signal contras between specular and diffuse reflection was tested as seen in figure 32. To test the behavior in these set-ups, the photodiode was first positioned so that the monitoring beam was reflected directly from the workpiece in to the diode, in a specular reflection. Secondly, the diode was positioned to the side of the monitoring beam plane, in order to detect the diffuse reflections given off by the workpiece. In both cases the monitoring beam was positioned outside of the scan head, in an angle to the work peace, as seen in figure 33.

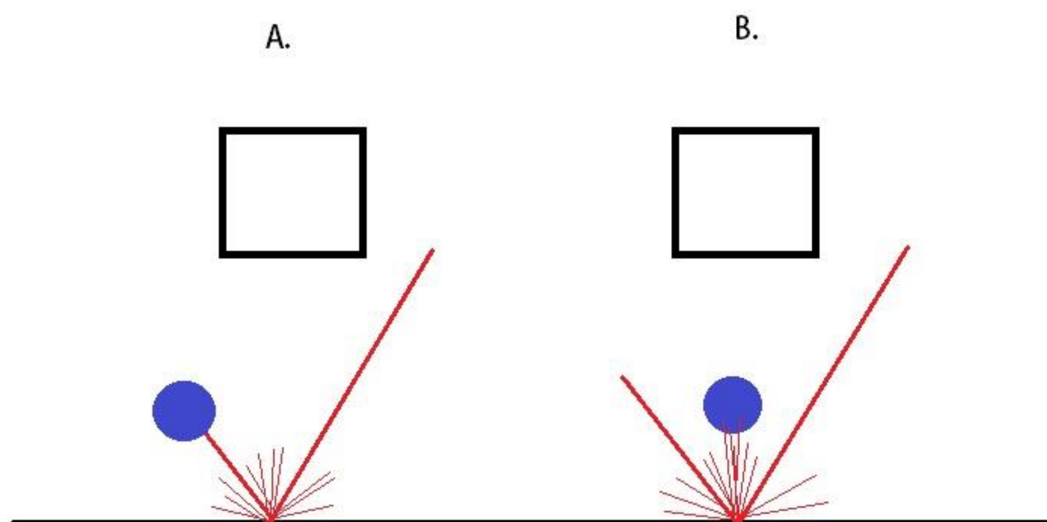

Figure 33. Specular (left) and diffuse (right) reflection observation. The blue dot represents the monitoring diode.

This experiments was conducted by moving test pieces of different materials, which had prescribed lines of varying width on their surface, across the monitoring beam path. Tested materials included samples of CIGS and anodized aluminum. The scribe width on the CIGS samples was approximately 50 µm.

8.2 CIGS Layer Distinction

To test the ability to distinguish between the different layers of a sample of scribed CIGS, the same testing setup was used as in specular versus diffuse reflection test (Figure 13). This time using only CIGS samples which were scribed to different depths. The principle of layer distinction based on layer reflectivity is illustrated in figures 34 and 35.

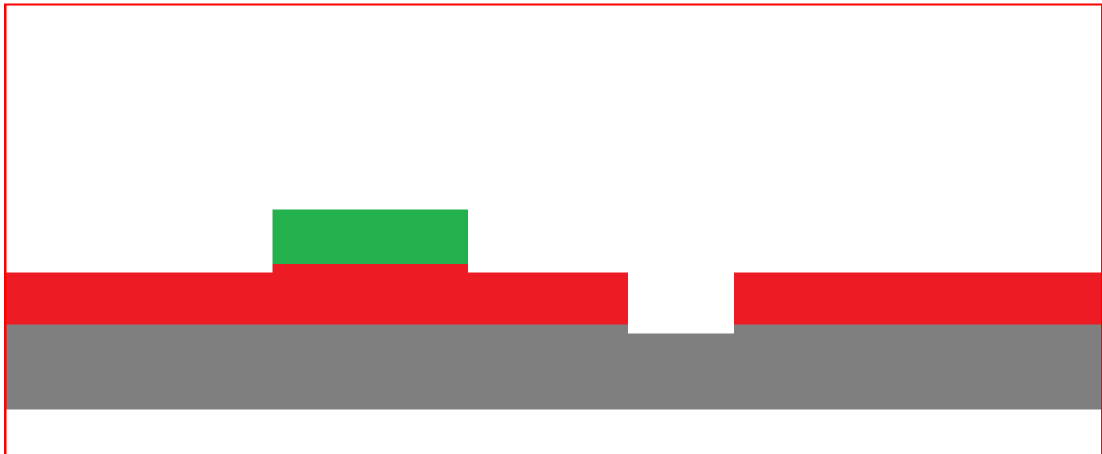

Figure 34. Diagram of test surface. Green: intact surface, red: second layer, grey: base layer.

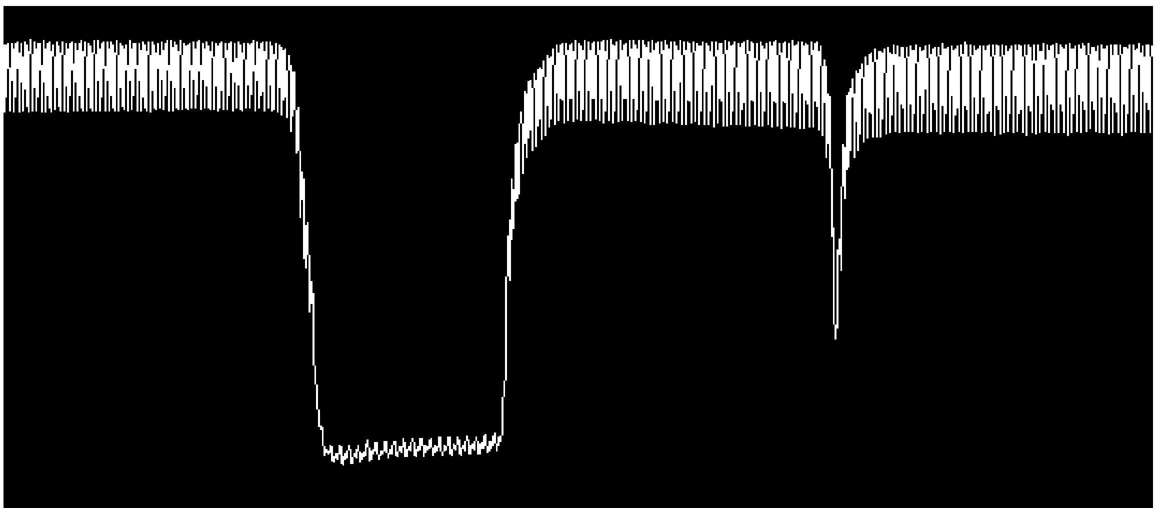

Figure 35. Reflected light intensity curve when going over test scribed surface.

Figure 34, shows a diagram of a layered sample material which has been mostly scribed to the depth of the second layer. There are defects in which either the top surface has been left intact, or in which the scribe has penetrated all the way to the base layer. In figure 35, we can see that the level of reflectivity is different between layers. In this case the second layer is the most reflective. When going over the intact surface, there is a pronounced drop in reflectivity, in comparison to the second layer. Also when going over the section which has penetrated to the base material, there is also a drop in reflectivity, but this drop is les in magnitude in comparison to the intact surface layer. In such a case it would be relatively simple to distinguish to which depth the scribe has penetrated.

8.3 Monitoring Setup Experiments

In order to trace the scribing line, the monitoring diode must be placed in position to view the relevant working area. This can be done either by having a diode pointed at the working area from outside of the scribing scan head, or by viewing the working area thru the scan head itself. These monitoring setups are shown in figure 36.

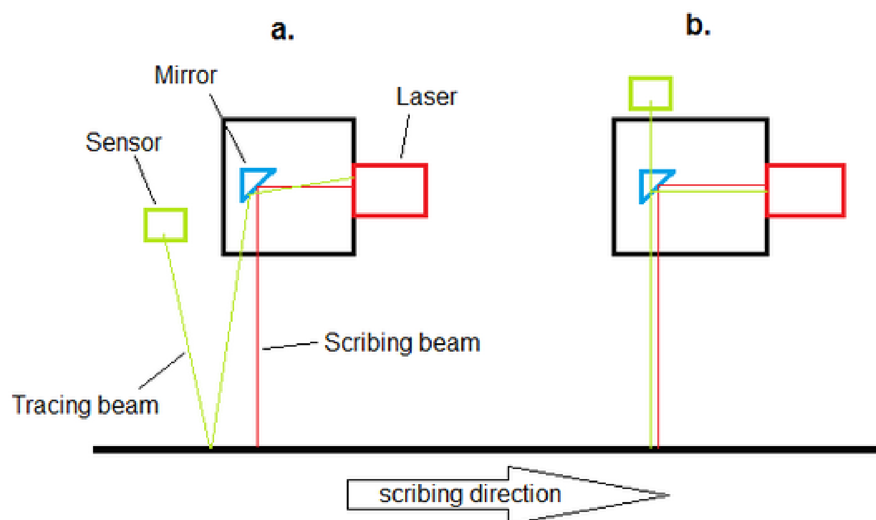

Figure 36. External and scan head integrated monitoring.

Both of these setups pose different challenges and benefits. The main difficulties in following the scribe path are: the difficulty of accurately following the scribe path with an externally mounted and independently moved diode, and the loss of reflected signal intensity when viewing thru the scan head.

The monitoring setup (a.) in figure 36, was constructed by placing the photodiode in an external clamp and focused on the relevant area. Setup (b.) in the same image was constructed by focusing the diode on the target area thru the scan head camera adapter. With the use of the dichromatic reflector of the scan head camera adapter, setup (b.) allows for the target to be viewed along the path of the actual scribing laser. The principle of monitoring setup (b.) is illustrated in greater detail in figure 37.

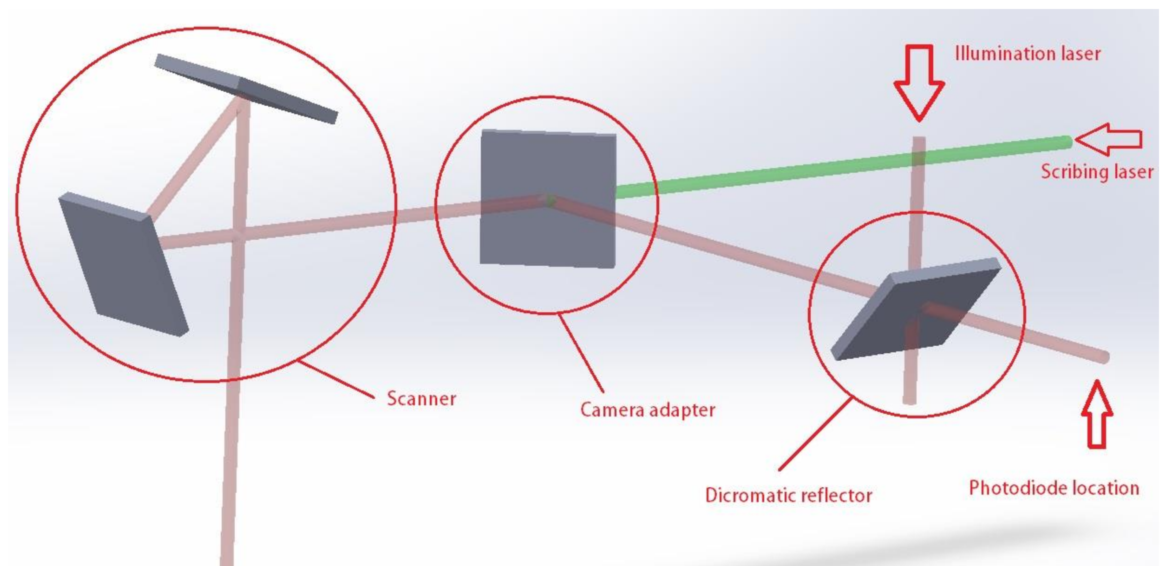

Figure 37. Illustration of the beam path thru the scribing laser assembly.

The experiment setup seen in figure 37, functions as follows. On the left the scanner with two (2) articulated fully reflective mirrors which direct the beam. In the middle, the "camera adapter" with a dichromatic mirror which allows the scribing beam to pass, but reflects the illumination. On the right a 50:50 dichromatic mirror which partially reflects the illuminating beam and partially allows it to pass. The illumination laser comes in to the mirror from above. A portion of the returning beam is projected on to the photodiode in the far right.

The experiments were conducted by sweeping over pre-scribed lines on a Cr-glass surface. The approximate thicknesses of the used lines are from 130 µm to 40 µm in 10µm increments accurate measurements are presented in the results. This was done to test if a beam reflected back thru the scanner was is a viable option for photodiode monitoring.

9 EXPERIMENTAL RESULTS

In this section we will go through the main points of the experimental results, including the Laser Welding Monitor tests as well as the various monitoring experiments made on our own system. The following topics contain the key results and information obtained from those experiments.

9.1 PRECITEC LWM tests

Some initial testing was carried out to test the usability of a commercially available system for this application. The PRECITEC LWM Laser Welding Monitor presented in a previous section was used for this purpose.

As seen in figure 38, when the sensor finds a scribing deflection the sensor output jumps to max (10). The sensor output on areas with correct scribing is always less than maximum. With this approach we can find the deflection n the scribe in real-time.

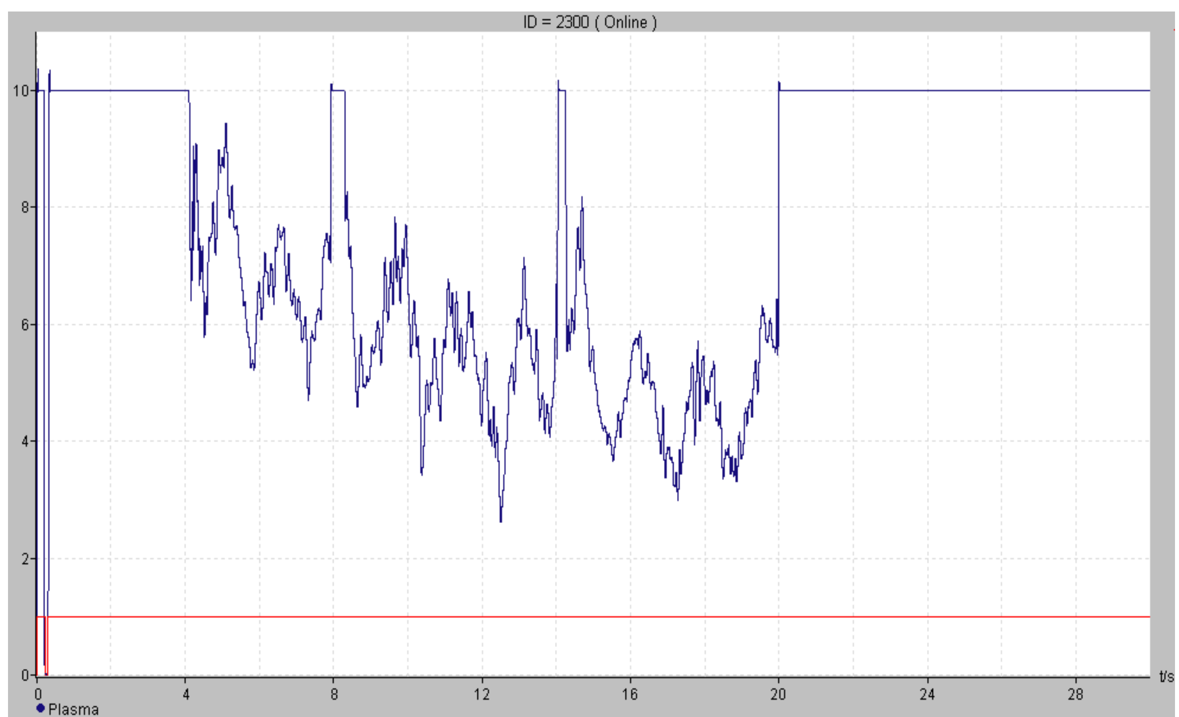

Figure 38. LWM photodiode output signal.

As seen in the figure, the LWM is capable of detecting defects in a workpiece, but its maximum sampling rate of 20 kHz was not adequate to be used in the monitoring of laser scribing, since it is a much faster process than laser welding. Therefore this approach was abandoned in favor of a more capable system.

9.2 Specular and Diffuse reflection

With the specular reflection the received light intensity was greater, but it was more difficult to align and would cause significant problems when monitoring a moving process. The diffuse reflection measurement was easier to align and game more reliable results. A diffuse reflection set-up would also be easier to configure for monitoring a moving scribe.

Figure 39 shows some samples of the CIGS material used in the experiments. Note that the lines in the picture that are highlighted by the square, are the specific lines used for the experiments that are discussed in further detail below.

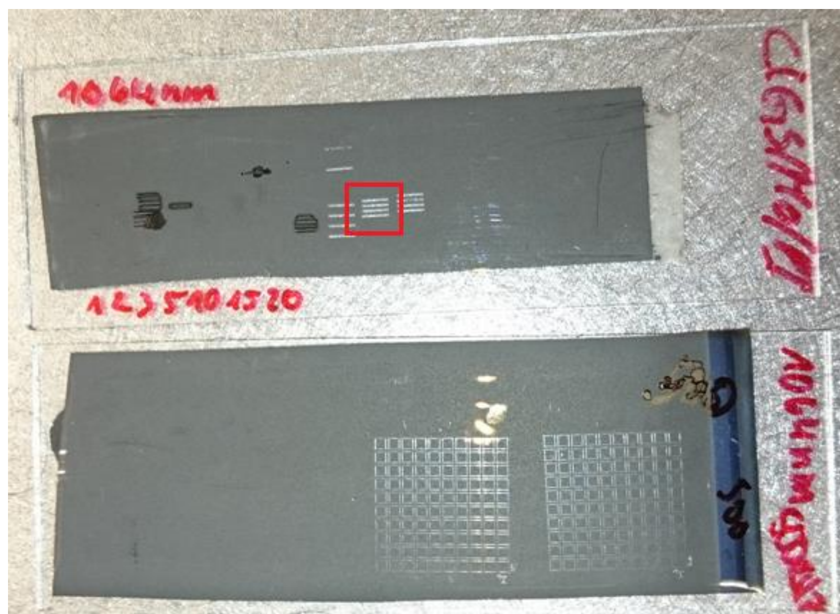

Figure 39. Some CIGS samples used for monitoring experimentation. The lines highlighted by the square where used for the specular vs. diffuse reflection experiments.

In figure 40, we can see the photodiode measurement, going over the CIGS sample with 4 lines shown in figure 39. There is a noticeable rise in reflectivity when crossing from the intact surface to over the first line. Also there are 4 discernible peaks, which correspond with the scribes.

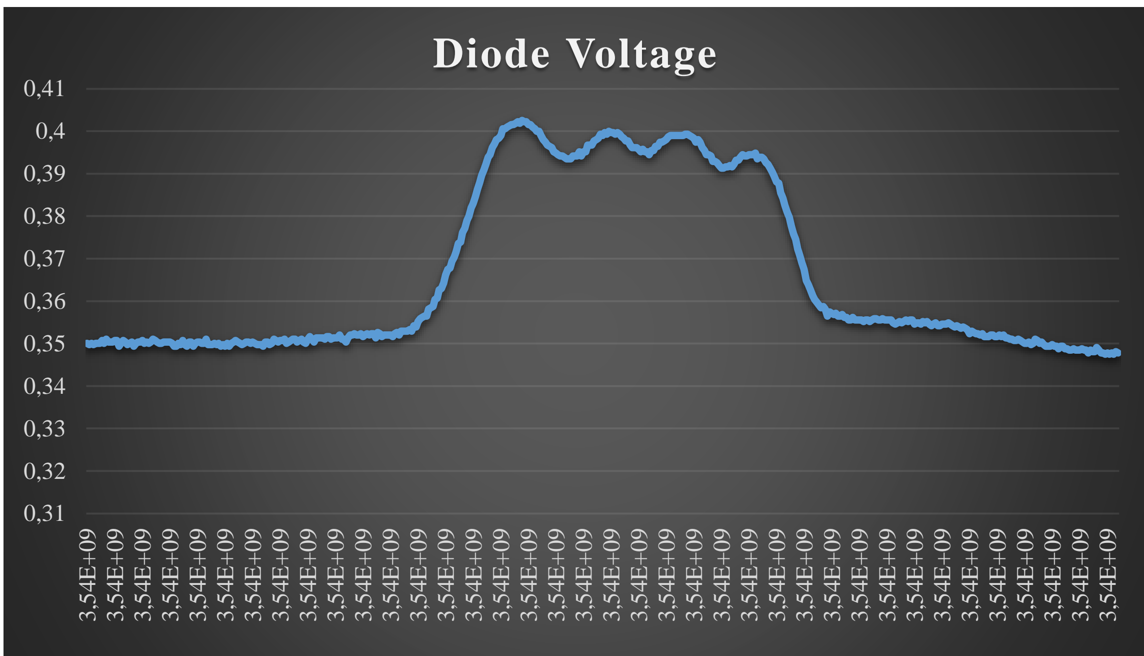

Figure 40. Photodiode induced voltage over time.

In figure 41, we also have 4 peaks. But this time they are seen as drops in light intensity. While the difference in intensity between the scribed and intact surface less than with the specular reflection, the contrast between lines is clearer.

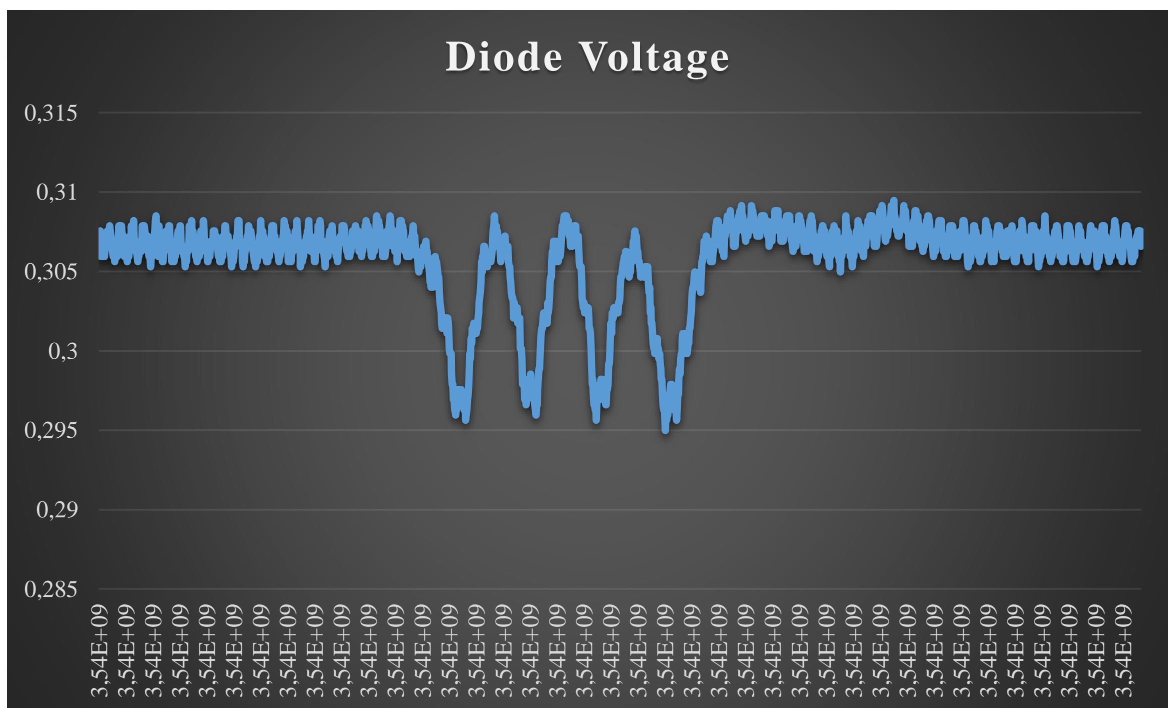

Figure 41. Photodiode induced voltage over time.

9.3 CIGS Layer Distinction

Some success was achieved with distinguishing between different CIGS layers based on their reflectivity. A distinction could be observed between lines that were scribed to different depths, crossing to the different layers. The notable difference in reflectivity between the layers of a CIGS sample allow for layer distinction under test circumstances. As the contrast between layers is proportional to the reflected intensity, it can be improved by modifying motoring beam parameters.

9.4 Monitoring Setup Experiments

The images below show the microscope images (figures 42-51) of the lines which were used in the experiments, along with the corresponding oscilloscope measurements. Note that the monitoring beam reciprocates over the line, so there is a periodically repeating curve. One period of the curve is a single pass over the line. The experiment described in this document was conducted to test the possibility of using photodiode detection with a monitoring beam projected and reflected thru the scanner, and based on the results, it appears that this is strong possibility.

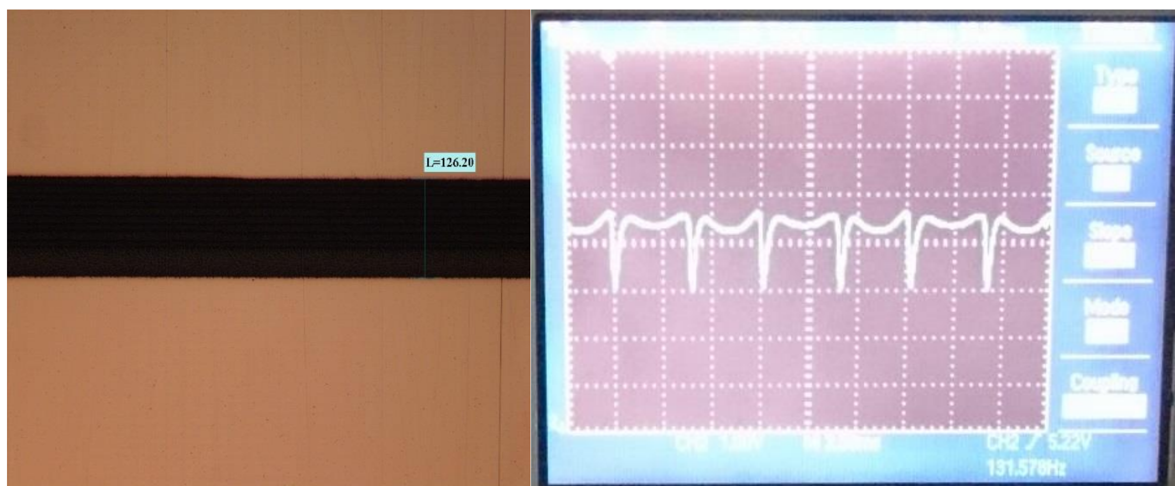

Figure 42. 126.20μ scribe and oscilloscope measurement.

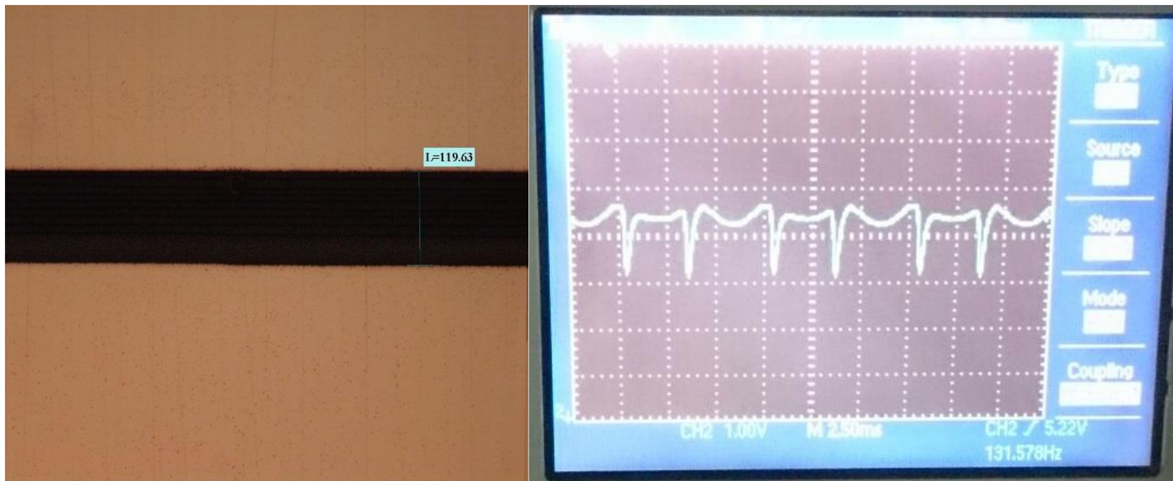

Figure 43. 119.63µ scribe and oscilloscope measurement.

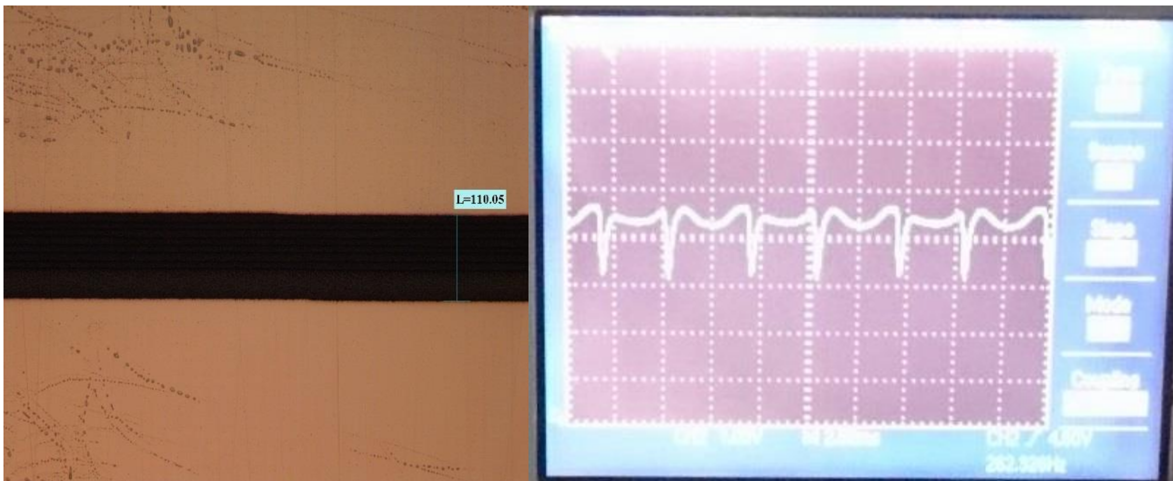

Figure 44. 110.05µ scribe and oscilloscope measurement.

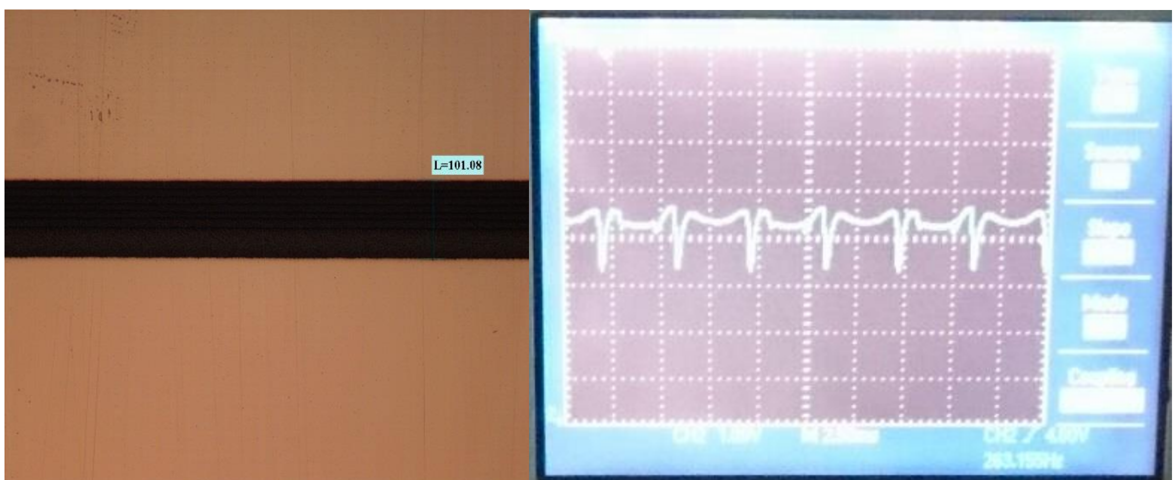

Figure 45. 101.08µ scribe and oscilloscope measurement.

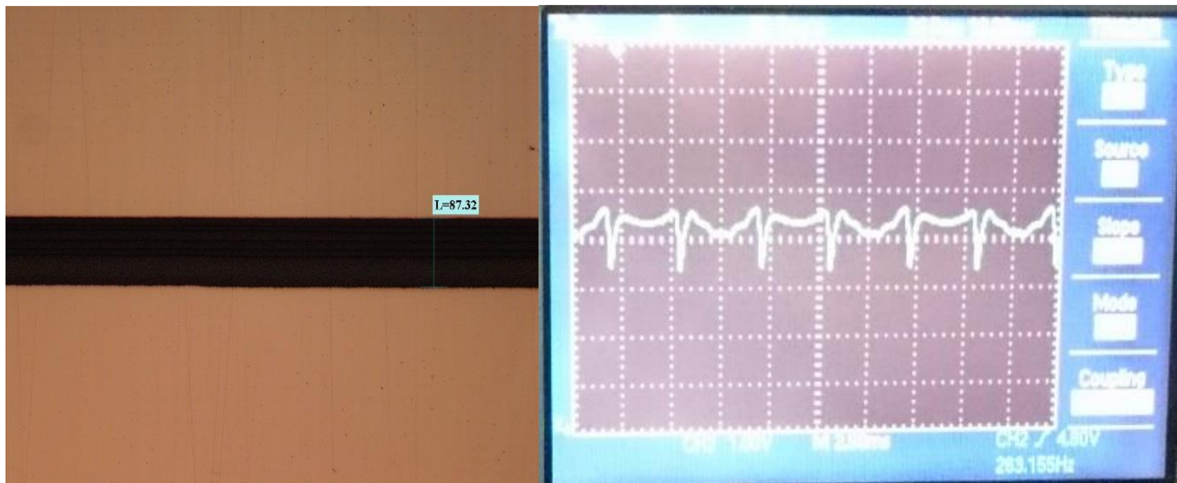

Figure 46. 87.32µ scribe and oscilloscope measurement.

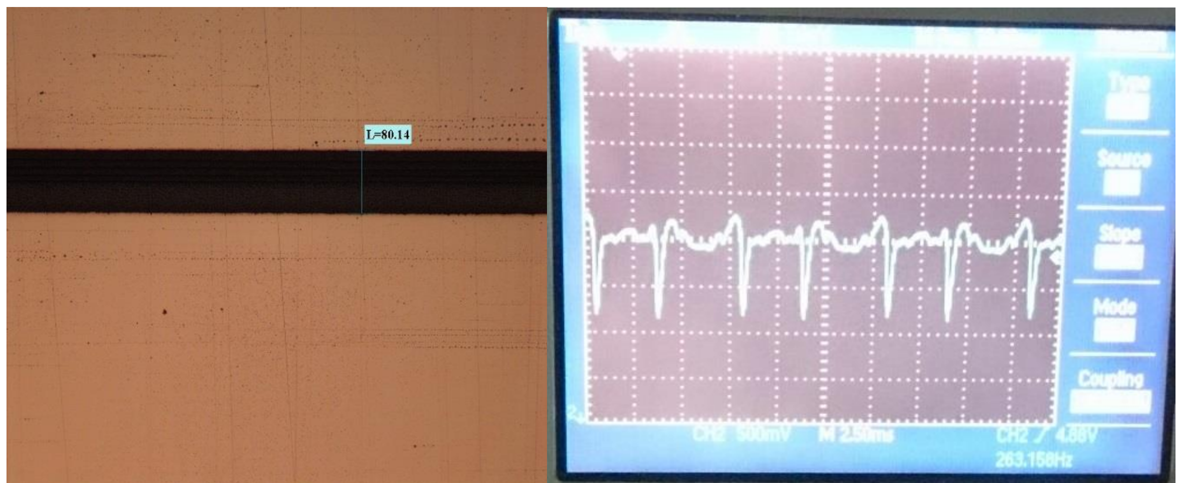

Figure 47. 80.14µ scribe and oscilloscope measurement.

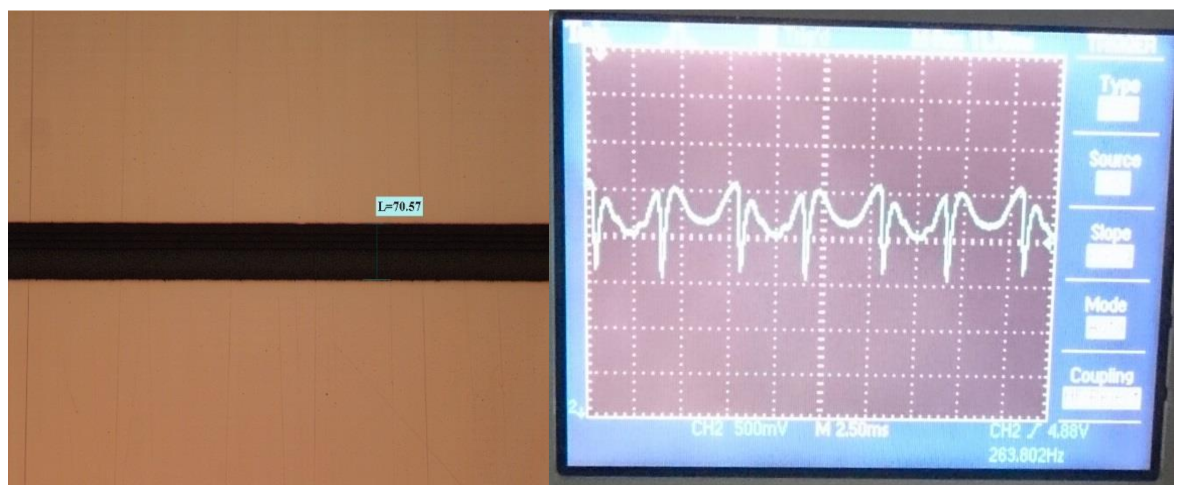

Figure 48. 70.57µ scribe and oscilloscope measurement.

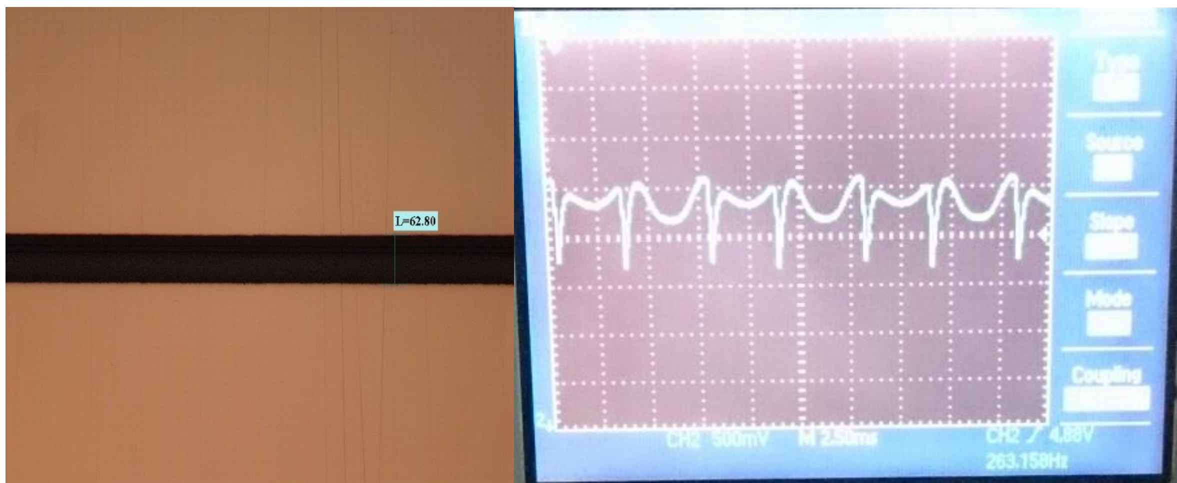

Figure 49. 62.80μ scribe and oscilloscope measurement.

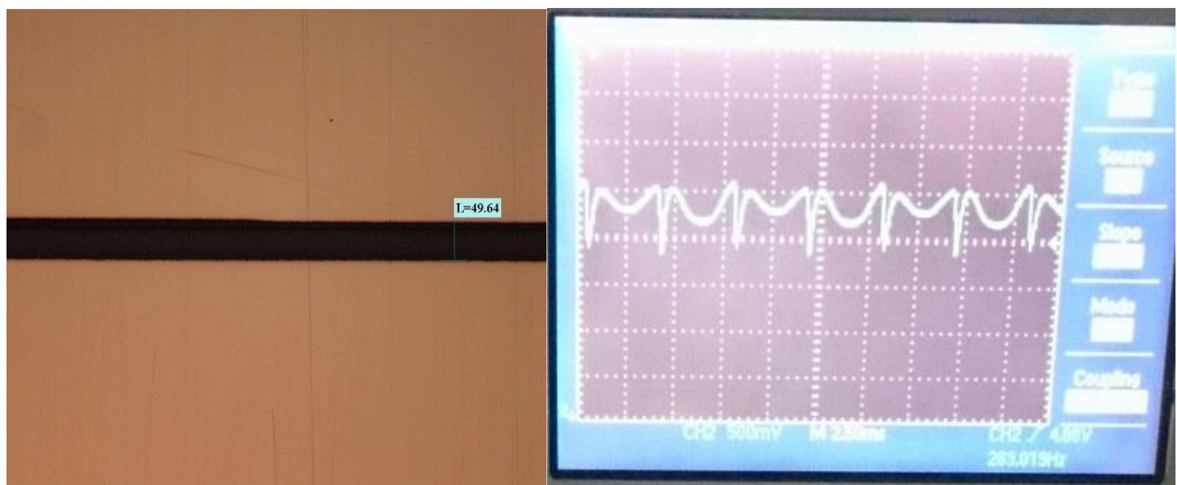

Figure 50. 49.64μ scribe and oscilloscope measurement.

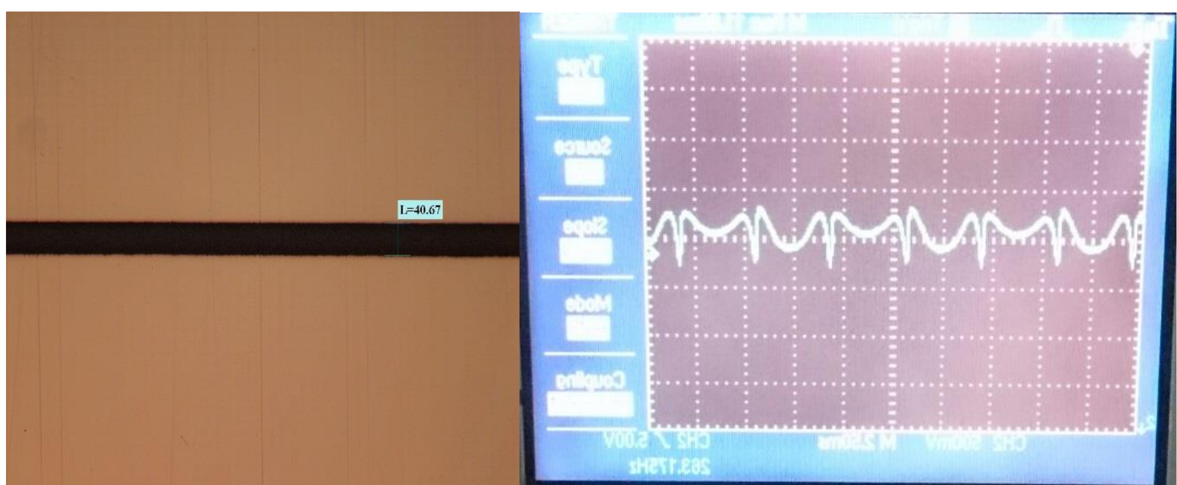

Figure 51. 40.67μ scribe and oscilloscope measurement.

10 ANALYSIS AND DISCUSSION

In principle this monitoring set-up works well, but as the line thickness decreases, so does the contrast between the scribed and the unscribed surface. Increasing the brightness of the illumination and optimizing the illumination beam and photodiode combination would produce better results, with better capability on different less reflective materials.

There is a noticeable change in intensity even over the unscribed surface due to the movement of the laser. As the beam moves in and out of the center position there is a correlating change in the returning beam intensity. Repeating the experiment with completely unscribed surface would yield a curve with a local maximum in the approximate position of the scribes. All of these factors need to be taken into account when designing a system based on this technology.

The concept is a promising one. It allows the greatest amount of laser movement compared to other photodiode monitoring setups. With an optimized combination of components the losses in the intensity of the returning beam could be overcome. There is also the possibility that when working with materials that are partially transparent, especially after scribing, that an illumination source projected thru the workpiece could be used to provide good contrast.

Overcoming optical errors in following the cribbing event is the greatest challenge in developing the system. A method for compensating for divergence in the operating field of the scribing laser is essential for the functioning of a monitoring system. The nature of the process and the speeds at which it operates mean that reflection contrast is the only option for distinguishing between layers. Maximizing contras while eliminating outside interference is also a limiting factor. As such the method is limited to certain material options and operating ranges.

11 CONCLUSIONS AND SUMMARY

The goal of this research was the testing and evaluation the applicability of commercially available photodiode and monitoring technology for the real-time monitoring of a laser scribing process.

The theoretical portion focused on gathering information about the operation of photodiodes in a sensor application. The relevant properties of different reflection types affecting the performance were also studied. This knowledge was applied in designing the experimental setups. Some research was also carried out on developing an analysis algorithm, but this was omitted in favor of finding an optimal detection solution. The gathering of knowledge on laser scribing technology as well as the study of existing laser-monitoring applications was also an important part of the process. An apparent conclusion was that, existing monitoring systems are typically designed for, and implemented in monitoring of relatively slow laser processes, such a laser welding, where the speed of the process does not pose a challenge for monitoring. The operating speed of existing monitoring applications is too slow for implementation in real-time monitoring in laser scribing applications, which operate at much greater speeds. This is why existing monitoring systems cannot be applied, and a new system must be developed for dealing with these faster operating speeds. This type of technology promises to provide increased efficiency in both manufacturing as well as operation in high accuracy, high speed low heat delivery manufacturing applications. As in solar cell manufacturing for example.

The experimental portion of the study focused on designing and testing different monitoring setups for real-time photodiode monitoring. A high performance PXI-system was built for handling the monitoring process. The system was designed to be used as the core for an integrated system of monitoring applications, where the photodiode monitoring would be used in conjunction with other monitoring methods. The additional methods including high-speed camera and spectrometer monitoring devices.

The goal these experiments was to evaluate the feasibility of applying photodiode monitoring to a laser scribing process, and identifying the key aspects for use in a real-time

monitoring application. For the purposes of monitoring a scribing process by detecting defects during the laser processing, the key factors are the reflectivity contrast between workpiece layers and the ability to precisely follow such a fast process with adequate accuracy. Currently available monitoring systems are capable of sampling rates on the order of ~25 kHz, but for adequate performance in laser scribing applications, a sampling rate of above 1 MHz would be required. Future developments would include identifying the proper operating wavelength for the illumination laser and photodiode pair for a given material, to minimize interference from other light sources and maximize contrast between scribed and unscribed surface. Also the photodiode observation path should be equally optimized to be able to follow the process at speed without significant loss in received intensity. At the current level of technology this type of monitoring process is very limited, but with adequate system development and optimization it could be utilized for specific manufacturing processes.

LIST OF REFERENCES

APPOLO Newsletter, Issue 1. [I4MS website] Published 28.2.2014. [Referred 14.4.2016] Available: http://i4ms.eu/difusion/appolo/news_feb.pdf?cv=1&session-id=a52fa3d9f069d39ce60169076feafd41

APPOLO project website. [APPOLO project website]. [Referred 5.5.2016]. Available: http://www.appolo-fp7.eu/

Photodiode Theory of Operation. [AP Technologies website]. [Referred 12.5.2016]. Available: https://www.aptechnologies.co.uk/support/photodiodes/photodiode-theory-of-operation

Burn, A., Romano, V., Muralt, M., Witter, R., Frei, B., Bücheler, S. & Nishiwaki, S. 2012. Selective ablation of thin films in latest generation CIGS solar cells with picosecond pulses. SPIE. 17 p.

Eberhardt, G., Banse, H., Wagner, U. & Peschel, T. 2010. Structuring of thin film solar cells. SPIE. 10 p.

Interface Specification YLP series Ytterbium Pulsed Fiber Lasers Interfaces “type D” and “type D1”. 2009. IPG Laser. 29 p.

Specification Ytterbium Pulsed Fiber Laser YLPM-1-4x200-20-20. 2009. IPG Laser. 3 p.

Helium-Neon Laser Heads 1100 Series. 2005. Edinburgh: JDS Uniphase. 5 p.

LabVIEW [National Instruments website]. [Referred 20.8.2016]. Available: www.ni.com/labview/

Laser Scribing Eases the Further Mechanical Processing [Rofin website]. [Accessed 16.3.2016]. Available: https://www.rofin.com/en/applications/laser-structuring/laser-scribing/

Liu, Z., Ukida, H., Niel, K. & Ramuhalli, P. 2015. Integrated Imaging and Vision Techniques for Industrial Inspection: Advances and Applications. London: Springer. 540 p.

Lucas, L. & Zhang, J. 2012. Femtosecond laser micromachining: A back-to-basics primer [Industrial Laser Solutions for Manufacturing website]. Published 1.6.2012. [Referred 16.3.2016]. Available: http://www.industrial-lasers.com/articles/2012/06/femtosecond-laser-micromachining-a-back-to-basics-primer.html

NI PXIe-1071 User Manual. 2013. National Instruments. 63 p.

NI BNC-2120. [National Instruments website]. [Referred 4.8.2016]. Available: http://sine.ni.com/nips/cds/view/p/lang/fi/nid/10712

BNC-2120 Installation Guide. 2012. National Instruments. 19 p.

PXIe-6363. [National Instruments website]. [Referred 4.8.2016]. Available: http://www.ni.com/fi-fi/support/model.pxie-6363.html

NI PXIe-6363 Device Specifications. 2015. National Instruments. 26 p.

NI PXIe-8880 User Manual. 2015. National Instruments. 71 p.

Nave, R. 2012 HyperPhysics Photodiode. [HyperPhysics website]. [Referred 25.4.2016]. Available: http://hyperphysics.phy-astr.gsu.edu/hbase/electronic/photdet.html

Laser Welding Monitor LWM - system description [PRECITEC website]. [Referred 7.3.2015]. Available: http://www.precitec.de/en/products/joining-technology/process-monitoring/laser-welding-monitor/?cv=1&session-id=c9de3303acaec362d5108e6301bbd32c

Purtonen, T., Kalliosaari, A. & Salminen, A. 2014. Monitoring and Adaptive Control of Laser Processes. Physics Procedia; 8th International Conference on Laser Assisted Net Shape Engineering LANE 2014, 56, pp. 1218-1231.

Rekow, M., Murison, R., Panarello, T., Dunsky, C., Dinkel, C., Nikumb, S., Pern, J., Mansfield, L. 2010. CIGS P1, P2, P3 Scribing Processes using a Pulse Programmable Industrial Fiber Laser. 13 p.

SCANLAB website [SCANLAB website]. [Referred 16.2.2016]. Available: http://www.scanlab.de/en/products

Steen, M.W. & Mazumder, J. 2010. Background to Laser Design and General Applications. London: Springer. 345 p.

APPENDIX I

Technical measurements and installation drawings for the monitoring adapter and its attachment to the scan head.